



**HAL**  
open science

## Review on frosting, defrosting and frost management techniques in industrial food freezers

Deyae Badri, Cyril Toublanc, Olivier Rouaud, Michel Havet

### ► To cite this version:

Deyae Badri, Cyril Toublanc, Olivier Rouaud, Michel Havet. Review on frosting, defrosting and frost management techniques in industrial food freezers. *Renewable and Sustainable Energy Reviews*, 2021, 151, 10.1016/j.rser.2021.111545 . hal-03392196

**HAL Id: hal-03392196**

**<https://hal.science/hal-03392196>**

Submitted on 22 Aug 2023

**HAL** is a multi-disciplinary open access archive for the deposit and dissemination of scientific research documents, whether they are published or not. The documents may come from teaching and research institutions in France or abroad, or from public or private research centers.

L'archive ouverte pluridisciplinaire **HAL**, est destinée au dépôt et à la diffusion de documents scientifiques de niveau recherche, publiés ou non, émanant des établissements d'enseignement et de recherche français ou étrangers, des laboratoires publics ou privés.



Distributed under a Creative Commons Attribution - NonCommercial 4.0 International License

# Review on frosting, defrosting and frost management techniques in industrial food freezers

Deyae BADRI<sup>(a)</sup>, Cyril TOUBLANC<sup>(a)</sup>, Olivier ROUAUD<sup>(a)</sup>, Michel HAVET<sup>(a)</sup>

<sup>(a)</sup> Oniris, Université de Nantes, CNRS, GEPEA, UMR 6144, F-44000 Nantes, France.

## Abstract

This paper reviews the results of frosting, defrosting and frost management research that have been reported over the past fifty years. The literature can be split into three categories: frost formation and properties, frost effect and frost management techniques, and those for different geometries and under different conditions. The aim is to provide an overview of the studies made over recent years that have targeted frost management, so researchers, manufacturers, designers and any concerned party can quickly obtain essential and sufficient information about the frosting phenomenon, allowing them to develop and complete ongoing studies. Emphasis is placed on analyzing available experimental, theoretical and numerical studies in industrial food freezing conditions. The specificities, constraints and challenges of industrial freezing are discussed in each section. Under industrial freezing conditions, several sources of humidity are involved and a third mechanism of frost formation in the air, may occur, resulting in less dense and more insulating frost. Numerical modeling has shown promising results in frosting/defrosting but other major parameters still need to be modeled in order to represent the real behavior of industrial systems. Evaporator-fan coupling must be taken into account as well as the need for a dynamic system approach. Many frost formation retardation and defrosting strategies may not provide the same effectiveness in these conditions compared to others. Several preventive, technical and research solutions have yet to be found. In this review, the gaps existing in research on frost in industrial food freezing conditions are identified, and recommendations are provided.

## Keywords

Food freezing, deep-frozen food, industrial freezer, finned tube, frosting, defrosting, food quality

## Nomenclature

A	Area (m <sup>2</sup> )
A <sub>w</sub>	water activity ( $= \frac{p_v}{p_{sat}}$ )
c <sub>a</sub>	specific heat capacity of air (J.kg <sup>-1</sup> .K <sup>-1</sup> )
C <sub>vap-eq</sub>	water vapor concentration in equilibrium with the product surface (kg.m <sup>-3</sup> )
C <sub>vap-sur</sub>	water vapor concentration in the surrounding air (kg.m <sup>-3</sup> )
D <sub>h</sub>	hydraulic diameter (m)
E	energy transfer coefficient (W.m <sup>-2</sup> . K <sup>-1</sup> )
F <sub>o</sub>	Fourier number ( $F_o = \frac{\alpha_a t}{D_h}$ )
h <sub>m</sub>	external mass transfer coefficient (m.s <sup>-1</sup> )
Δh	latent heat of condensation or sublimation of water vapor (J.kg <sup>-1</sup> )

$k$	thermal conductivity ( $\text{W}\cdot\text{m}^{-1}\cdot\text{K}^{-1}$ )
$\dot{m}$	mass flow rate ( $\text{kg}\cdot\text{s}^{-1}$ )
$m''$	mass concentration ( $\text{kg}\cdot\text{m}^{-2}$ )
$\dot{m}''$	mass flux ( $\text{kg}\cdot\text{s}^{-1}\cdot\text{m}^{-2}$ )
MRI	frost mass reduction Index
P	pressure (Pa)
$Q_v$	air volume flow rate ( $\text{m}^3\cdot\text{s}^{-1}$ )
$r_E$	coil air-on absolute humidity ( $\text{kg}\cdot\text{kg}^{-1}$ )
$r_S$	coil air-off absolute humidity ( $\text{kg}\cdot\text{kg}^{-1}$ )
SHR	sensible heat ratio ( $= \frac{\phi_{sens}}{\phi_{sens}+\phi_{lat}}$ )
T	temperature (K)
U	heat transfer coefficient ( $\text{W}\cdot\text{m}^{-2}\cdot\text{K}^{-1}$ )
UA	sensible capacity rating ( $\text{W}\cdot\text{K}^{-1}$ )
V	velocity ( $\text{m}\cdot\text{s}^{-1}$ )
t	time (s)
$x$	distance from the leading edge of the test plate (m)
$x^*$	dimensionless position ( $= \frac{x}{D_h}$ )

### **abbreviation**

FPI	fins per inch
GHG	greenhouse gas
HVAC	heating, ventilation and air-conditioning
HGD	hot gas defrosting
IIR	International Institute of Refrigeration
RH	relative humidity
TD	air refrigerant temperature difference

### **Greek letters**

$\alpha_a$	thermal diffusivity of the air at the frost surface ( $\text{m}^2\cdot\text{s}^{-1}$ )
$\delta_{fr}$	frost thickness (mm)
$\theta$	temperature ( $^{\circ}\text{C}$ )
$\theta_E$	coil air-on temperature ( $^{\circ}\text{C}$ )
$\theta_S$	coil air-off temperature ( $^{\circ}\text{C}$ )
$\rho_{fr}$	frost density ( $\text{kg}\cdot\text{m}^{-3}$ )
$\phi_{lat}$	latent heat load (W)
$\phi_{sens}$	sensible heat load (W)
$\phi_{total}$	total heat transfer rate (W)
$\omega$	humidity ratio ( $\text{kg}\cdot\text{kg}^{-1}$ )

### **Subscripts**

a	air
adp	apparatus dew-point
e	on
evap	evaporation
fr	frost
ini	initial
lat	latent
m	mass
s	off
sat	saturated

sens	sensible
v	vapor, vaporization
w	water
0	dry conditions

## 1. Introduction

The use of refrigeration in the food sector is continually expanding to meet the needs of the population [1]. Most existing refrigerating equipment is based on the compression and expansion of a refrigerant. However, this compounds environmental issues. Indeed, refrigeration consumes about 15% of all electricity consumed worldwide, and the latter is mostly produced using fossil fuels [1]. Refrigeration is the major energy-intensive process of the food chain and, in high-income countries, it is the major contributor of GHG emissions in the postproduction food chain [2]. As promoted by IIR, reducing the energy consumption of refrigerating equipment must become a key environmental priority throughout the sector. The growth of the frozen food industry has also fueled the need for new technologies to improve freezing process efficiency and reduce its cost [3]. The freezing and storage of products at negative temperatures (below 0°C), are very widespread in the food industry because they contribute to maintaining product quality over long periods. Since a single-stage vapor-compression refrigeration system is insufficient for these low-temperature applications, refrigeration units are usually designed in two stages or in cascade.

In industrial and commercial practices, two temperature categories are adopted to describe either frozen food or deep-frozen food. The term frozen food is used for products which are maintained at a steady temperature of -10 °C or colder. These products are frozen by a technique which involves a slow decrease in temperature. The term deep frozen food is used when the products temperature rapidly reaches -18 °C and is maintained at this temperature or colder. These products are frozen by different techniques which involve rapid and sudden freezing, exposing them intensely to temperatures from -30 °C to -196 °C until the product core temperature reaches -18 °C. Thanks to this process, the water contained in the cells of the products is finely crystallized [4,5]. Thus, the treated products retain their freshness, textures and flavors, keeping their essential nutrients and vitamins. The deep-freezing process requires specific equipment which may be divided into the following main groups according to the heat transfer medium [6]: Direct contact (plate, band and drum freezers), air or other gaseous media (blast freezers), liquid (immersion freezers) and liquid/solid evaporation (liquid nitrogen and solid or liquid carbon dioxide freezers).

Air-blast freezers are the most common type of food freezer in which individual product items or cardboard products are placed in a forced air stream within a cabinet or tunnel. When the products are unpackaged, they release moisture due to the evaporation of water. Moreover, moist air can also enter into the freezer, especially from the freezer openings designed for the entry and exit of products (Figure 1). To ensure freezing, air is cooled through the evaporator and pulsed onto the product by fans at high-speeds ranging from 3 m/s to 6 m/s and at a temperature ranging from -25 °C to -40 °C or less, then it is recycled to be cooled again. Air blast freezers operate with an evaporator in the form of

a finned tube heat exchanger. Frost formation occurs when the air is in contact with the surfaces of cold coils whose temperature is below the dew point temperature of this air and the freezing point of water.

Whatever the engineering application, this frost deposition reduces the heat transfer between the air and the outer surface of the evaporator [7,8], decreases the airflow rate by up to 80% [9,10], greatly reduces the refrigeration system capacity [11] and may increase its energy consumption [12]. Subsequently, the impact of this energy consumption leads to an economic impact.

To avoid these negative consequences of frost formation, several frost management strategies and defrosting methods have been proposed and implemented [13]. Nevertheless, if these methods are not well conducted, they can penalize the efficiency of the systems used instead of improving their performance [14].

Optimizing defrost systems means adapting technologies to the type of frost formed and controlling their starting and stopping times. To do this, most researchers have focused on the formation mechanisms [15–17] and properties of frost [18]. Understanding the frost formation process and being able to predict the properties of the frost layer are both key elements required when proposing effective frost management solutions. The more the designers of heat exchangers are able to predict the dynamic of frost layer growth, the more they will be able to design a system to slow frost growth as much as possible and/or minimize the impact of frost on the energy performance of the whole unit. In the last few decades, many studies have been conducted on these different frosting and defrosting issues, but very few of them have placed this topic in the context of industrial food freezing. Most of them dealt with refrigeration and heat pump applications.

An industrial deep-freezer is more sensitive to frost phenomena compared, for example, to a heat pump or a simple domestic fridge. This is due to the combination of many different factors such as: very low temperatures, numerous sources of humidity, the complex geometry of the evaporators and also many constraints that can limit the application of frost management solutions. In addition, it should be noted that food quality is another important factor that has to be considered when evaluating the harmful consequences linked to the presence of frost in an industrial agri-food freezer.

Many interesting reviews have been written, summarizing and analyzing the literature on the frost formation process, frost characteristics [18], and defrosting technologies [13,19]. However, most of these reviews focused on one or two points or even on a particular case like a specific geometry [20] or specific and limited conditions [21].

The purpose of this article is not only to make an exhaustive presentation of the literature, but also to conduct, in a synthetic and clear way, a thorough study of all the issues linked to both frosting and defrosting processes. This review will help researchers, manufacturers, designers and any concerned party to obtain an overview of the various efforts made over the last 50 years in the area of frost management. These reported efforts include those concerning the frost formation process, frost growth and properties, the frost effect, and defrosting technologies. For each topic, attention is given to

industrial food freezers to highlight their particularities and challenges. Finally, conclusions are drawn and the outlook for the future is presented.

The present review is divided into four main sections. First, a synthetic database is proposed to know how the literature deals with frost issues in industrial freezing processes. In the second section, the frosting process is explained, focusing on the studies that have been carried out to examine the properties of frost and its growth under different conditions and for different applications. The third section is devoted to studies related to frost thermal and hydraulic effects. The last section is devoted to studies aimed at managing the problem of frost. At the end of each section, and by combining elements from the literature with the author’s knowledge, the particularities of the deep-freezing process are pointed out.

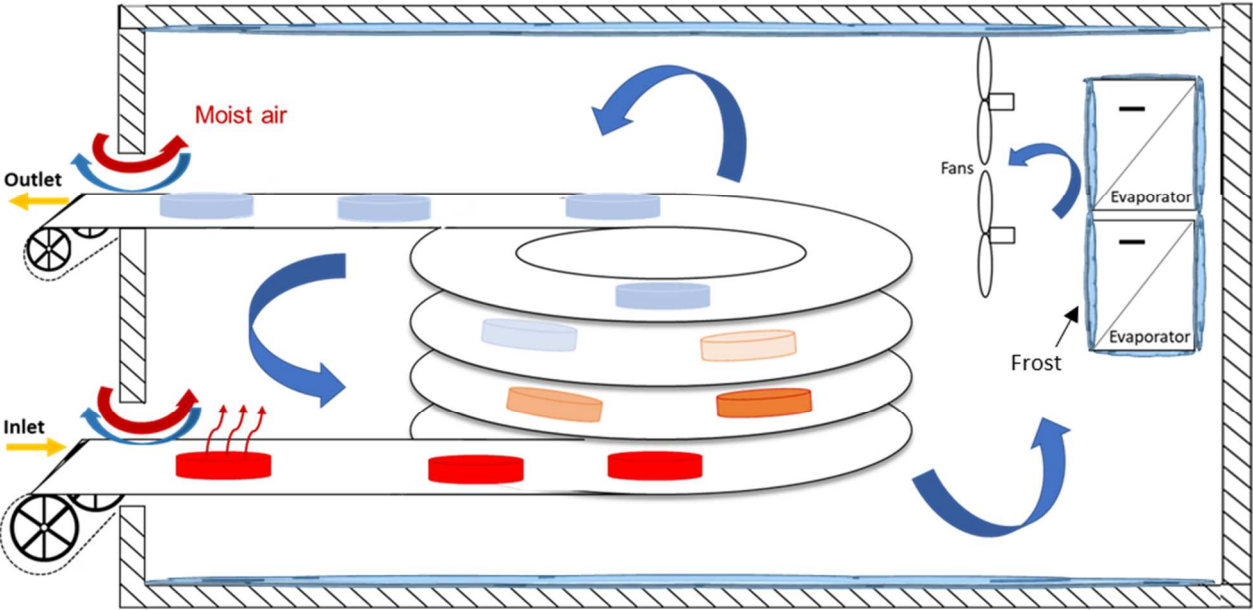


*Figure 1: Schematic of a spiral air blast freezer under frosting conditions.*

## 2. Preliminary overview of research on industrial freezing conditions

Based on the existing literature from the 1957 to 2020, a database of around 130 papers has been generated in order to categorize the studies carried out under freezing conditions and on an industrial scale compared to those carried out under other conditions (heat pump, HVAC, cryogenic, etc.) and at other scales (laboratory, domestic, etc.).

In the framework of the objective of this review, the literature which reported frosting and defrosting research in any conditions or applied to any field was selected. Then, the appropriate literature was classified by year of publication. Next, the literature was classified by:

- Type of studies: experimental or numerical/ theoretical;
- Type of geometry: simple geometry (flat plate, cylinder, parallel plates, vertical plate) or complex geometry (finned-tube, microchannel, etc.);
- Range of wall temperature and air inlet temperature;
- Range of air inlet velocity;
- Fan control mode: constant airflow (variable fan speed) or variable airflow according to fan curve.

Despite the clear progress made with the number of theoretical and numerical studies between 1957 and 2020 (Figure 2), experimental studies remain predominant and make up about 60% of the total studies. Different experimental configurations ranging from laboratory apparatus to industrial evaporators led to better understanding of many aspects of the phenomena involved. However, there are still some challenges and progress to be made relating to certain measurements (frost thickness, mass, distribution) and on data acquisition [22]. The lack of numerical studies, especially in the 20<sup>th</sup> century, may be explained by the complexity of the phenomena which are non-linear, transient and need the appropriate coupling of heat and mass transfer models with a wide range of boundary conditions. With the progress achieved in numerical tools, efforts have been made in recent years to take into account the maximum physical phenomena in modeling, adopt several approaches [23] and model complex geometries.

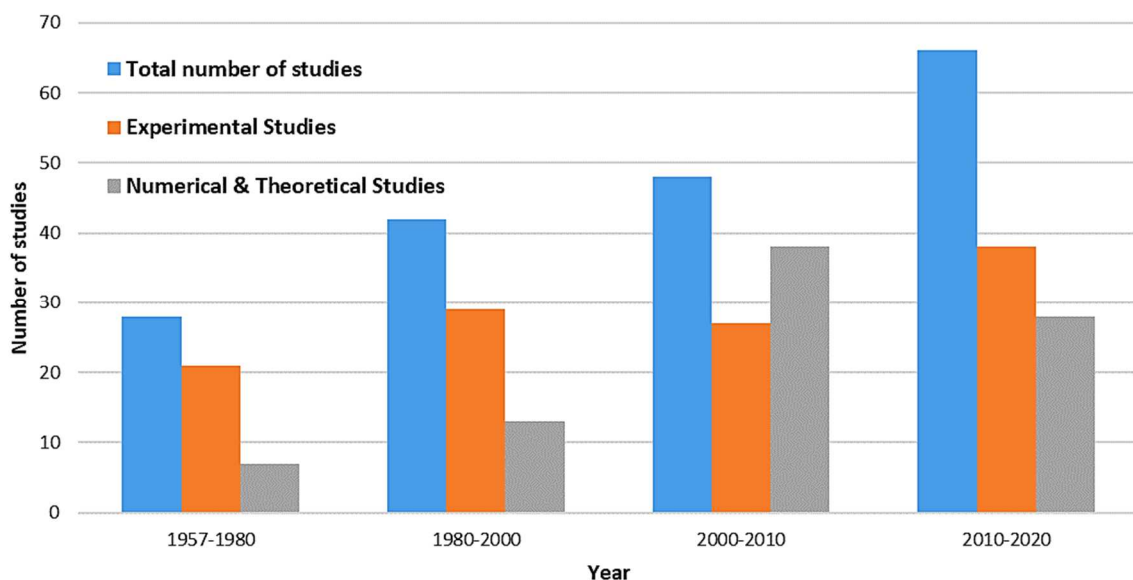


**Figure 2: Distribution of numerical and experimental works on frosting and defrosting published from 1950 to 2020.**

The type of surfaces that have been studied is shared almost equally between the simple surfaces and the complex surfaces of heat exchangers. However, in the latest review [18] reporting the literature up to around 2018, the authors noted that most studies prior to 2010 were focused on flat plate surfaces which are more basic. The review also showed that during the last decade the heat exchangers have received more interest.

Figure 3 (a) and Figure 3(b) clearly point out that, in the literature, the wall temperature and the air temperature mostly range between -15 to -5 °C and 0 to 20 °C, respectively. These ranges are easier to reproduce experimentally, but above all it confirms that most of the applications studied target heat pump applications.

It should be noted that low wall temperatures are not neglected in the same way as in recent decades. Recently, frost properties, the thermo-hydraulic behavior of the heat exchanger and defrosting have been investigated at temperatures below -30 °C. However, these wall temperatures have always been coupled to high air inlet temperatures in order to enrich the input data to understand the dynamics of frost. Nevertheless, they are not representative of real freezing conditions.

By categorizing studies by range of air velocity (Figure 4), it can be seen that around 60% of the total studies focused on low velocity < 2 m/s whereas only 20% of them focused on higher air velocities (> 3 m/s) such as encountered in industrial freezers.

To better examine the presence of freezing conditions in the frosting and defrosting literature, we selected only the studies that satisfy three conditions at the same time. These are: low wall temperature (<-30 °C), low air temperature, and high air velocity (>3 m/s). Doing this, some typical studies from the 1957 to 2020 and their operational geometries, temperature ranges, and air velocities are listed in Table 1; the data from the table are illustrated in Figure 5. Only 13% of all the research from 1957 to 2020 has investigated the problem of frosting/defrosting in freezing conditions, with simple and complex geometries. Adding complex geometry as the fourth condition, only 7% of total research has investigated a whole heat exchanger in freezing conditions. Despite the major challenges involved in controlling frost during deep freezing conditions, these figures indicate that the literature is rather poor in this area, therefore encouraging investigation.

In addition, almost all industrial freezing systems are equipped with a fixed-speed motor driven fan coil unit. But, the behavior of frost and its effects on evaporator thermal hydraulic performance will not be the same when operating with a variable fan speed to maintain a constant airflow [24]. Therefore, we have classified the literature by fan control mode. More than 80% of the studies were carried out at constant airflow (variable fan speed). Nonetheless, most of the studies, especially those using models, did not consider the decrease airflow that actually takes place in fan-supplied evaporators under frost conditions, which is one of the primary causes of cooling capacity reduction. Taking into account the fan-supplied airflow reduction, the air convective thermal resistance (due to frost blocking effect) in a heat exchanger may be 6 times higher than the conductive counterpart (due

the frost thermal resistance) after 75 minutes operating time [25]. Indeed, this condition of constant fan speed has been added to the selection criteria of industrial freezing conditions. According to the authors knowledge, only one existing study [26] has been carried out on the large air cooling evaporator coils typically used in an industrial ammonia freezing system operating under low air and refrigerant temperature conditions with a finned tube heat exchanger and high air velocity.

However, this study does not enrich the literature with complete data on the occurrence of frost under these conditions. It is only recently in 2020, that dynamic modeling and simulation were performed on a laboratory air blast freezer and showed promising results in this field [27]. Badri et al. [27] used a simple frost model based on a constant frost density ( $128 \text{ kg/m}^3$ ). Such simplification allows the prediction of adequate trends of frost properties. However, the frost effect on the thermo-hydraulic performance of the freezer would likely be confounded since assuming a constant frost density may cause an under-prediction of frost thickness especially during the early stage. Therefore, the model must be completed with other phenomena, mainly the water vapor diffusion inside the frost layer.

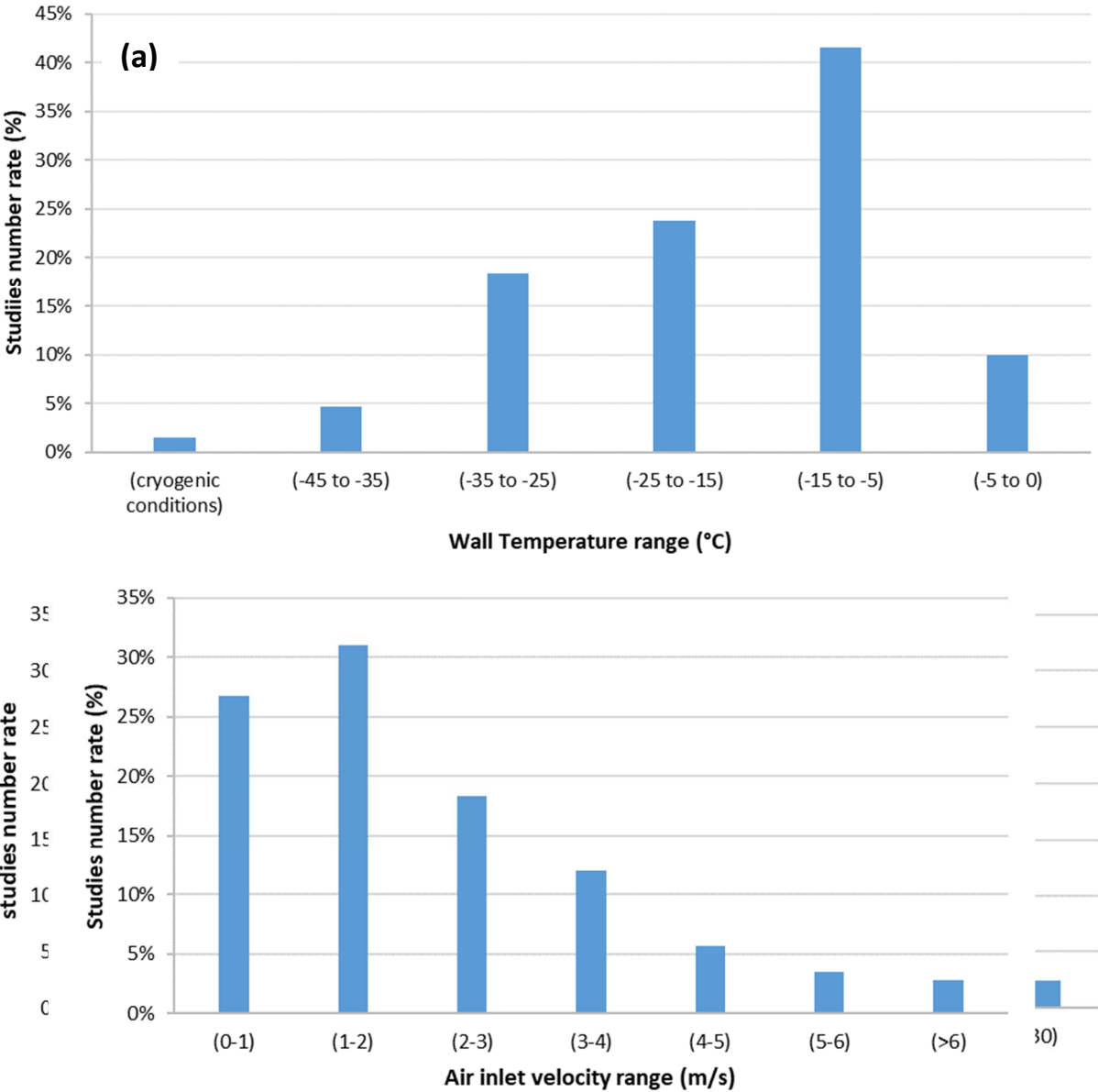


**Figure 3: Data analysis of Frosting/Defrosting studies (numerical and experimental) – (a) Wall Temperature range.**  
**Figure 4: Data analysis of Frosting/Defrosting studies (Numerical and Experimental) – Air inlet velocity.**

**Table 1: Experimental and numerical studies of frosting/defrosting under freezing conditions.**

Year	Scholars	Approach	Geometry	$\theta_a$ (°C)	$\theta_{wall}$ (°C)	$V_a$ (m/s)	Fan mode
1967	Lotz et al. [28]	Experimental	Finned tube	-20 to 0	-30	2.5	Constant
1989	Patin et al. [29]	Theoretical	-	-26	-30	-	-
1999	Chen et al. [30]	Numerical	Finned tube	-21 to -13	-41 to -31	4.4	Constant
1999	Mao et al. [31]	Numerical and Experimental	Flat plat	-10 to -26	-20 to -41	1 to 4	Constant
2000	Chen et al. [32]	Numerical	Flat plate	-21 to -13	-41 to -31	2	Constant
2001	Sherif et al. [33]	Experimental	Finned tube	-8.3	-40	3.81	-
2002	Verma et al. [34]	Numerical and Experimental	Finned tube	-20	-30	2.2	Constant
2004	Aljuwayhel et al. [35]	Experimental	Finned tube	-27	-34.5	3	Variable
2004	Seker et al. [36]	Numerical	Finned tube	-20	-35	3	Constant
2004	Seker et al. [37]	Experimental	Finned tube	-20	-35	3	Constant
2007	Aljuwayhel et al. [38]	Numerical	Finned tube	-27	-34.5	3	Variable
2008	Piucco et al. [39]	Numerical and Experimental	Flat plate	-20 to 30	-30 to 0	0.7 to 2	Constant
2009	Hermes et al. [40]	Experimental	Flat plate	-20 to 30	-30 to 0	0.7 to 2	Constant
2009	Cao et al. [41]	Numerical	Flat plate	-24	-39.22	1 to 4	Constant
2012	Wang et al. [42]	Numerical and Experimental	Flat plate	-8 to 19	-30 to 0	0.5 to 5	Constant
2018	Kumala et al. [43]	Experimental	Finned tube	-20	-40	-	-
2020	Badri et al. [27]	Numerical	Finned tube	-30	-35	3.6	Variable

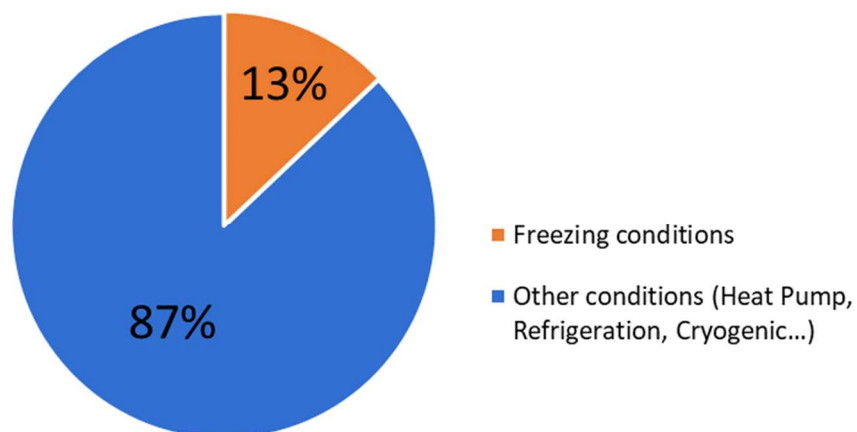


**Figure 5: Data analysis of Frosting/Defrosting studies (Numerical and Experimental) – Operating Conditions.**

### **3. Frost formation process, frost growth and frost properties**

Frost formation has received varying degrees of attention over the last 50 years. A large number of experimental, theoretical and numerical investigations have been reported relative to frost formation mechanisms, frost growth and frost properties. The different stages involved are studied sequentially to understand the whole frosting process and the factors affecting this phenomenon. Moreover, numerical models and empirical correlations have been proposed to predict frost properties in order to develop effective defrosting and anti-frosting technologies.

#### **3.1 Frost formation process**

Whatever the use of the heat exchanger, the two main factors that provoke frost formation on its surface are humidity and temperature. The difference resides in the transformation mechanism of the vapor contained in the air into ice crystals and the way it is deposited on the cold coils of the heat exchanger. Two studies by Hermes et al. [39,40] investigated frost formation on a cold plate and found that two types of transformations can occur:

- Either the vapor condenses in contact with the cold wall if the surface temperature is below the dew-point but higher than the triple point of water. Then, the droplets formed can freeze if the temperature of the surface decreases to 0 °C.
- Or the vapor turns directly into ice crystals (desublimation) in the case where the temperature of the surface and the dew-point are both lower than the triple point of the water.

Brian et al. [44] discussed another mechanism of frost formation. The air vapor may freeze in the air without any contact with a wall, thus forming a fog, before being deposited on the different cold surfaces in the freezer. These researchers explained that this phenomenon is due to the large temperature difference between the bulk air and the evaporator walls. The properties of the frost formed under these conditions are different from those of the frost formed by the two mechanisms described previously. This phenomenon will be discussed in more detail in section 3.3.

Moreover, as the way frost occurs on the plate can significantly influence its growth, some researchers have focused in particular on the analysis of the aspect of the ice crystals formed as a function of the air humidity and the temperature of the cold surface. Kobayashi [45] proposed a map of the different shapes of ice crystals formed under different temperature and super-saturation degree conditions. Qu et al. [46] took this idea further by adding that the shape of crystals subsequently influences the growth rate in the early stage of frost formation.

In Figure 6, a graph proposed by Wu et al. [47] shows the initial frost crystals classified into five groups according to their occurrence and shape. This classification has been obtained by observing the mesoscale frost formation process on a horizontal flat copper surface exposed to an airflow at 22 °C. As mentioned by Kobayashi [45], the appearance of crystals is not identical, reinforcing the idea that there is a relationship between crystal morphologies, the temperature of the cold plate and air humidity. We highlight that, using microscopy, some authors have observed that the shape of ice crystals is primordially affected by surface temperature and less affected by relative humidity.

Nevertheless, it should be noted that their experiments were carried out on surfaces ranging from -20 to 0 °C and in air at 22 °C. This means that at much lower temperatures the appearance of the crystals may be different, likewise for the effects of temperature and humidity.

Some researchers have studied frost formation on other different geometries. The studies of Lee et al. [48] on a vertical plate, Tajima et al. [49] on a vertical plate air cooler, Cremer and Mehra [50] on a cylinder, and Han and Ro [51] on parallel plates, have all enhanced the previous results relating to frost formation mechanisms. Moreover, these authors added that frost can be formed even under low humidity with a dew point below 0 °C, in agreement with the results of Wu et al. [47]. According to Han and Ro [51], location is an important factor to take in account during studies of frost formation mechanisms in complex geometries and especially for a finned tube geometry which is more disadvantageous regarding this aspect. Frost distribution is not homogeneous and therefore the test location cannot always be representative of the whole geometry.

Leoni [52] reinforced this idea and estimates that it is easier to study or visualize the frost formation process on flat plates microscopically and determine the key parameters involved in it. Other geometries were more difficult to study; this is due to several constraints, mainly the uniformity and the distribution of frost on these types of geometry as well as the difficulty of carrying out measurements on these evaporators.

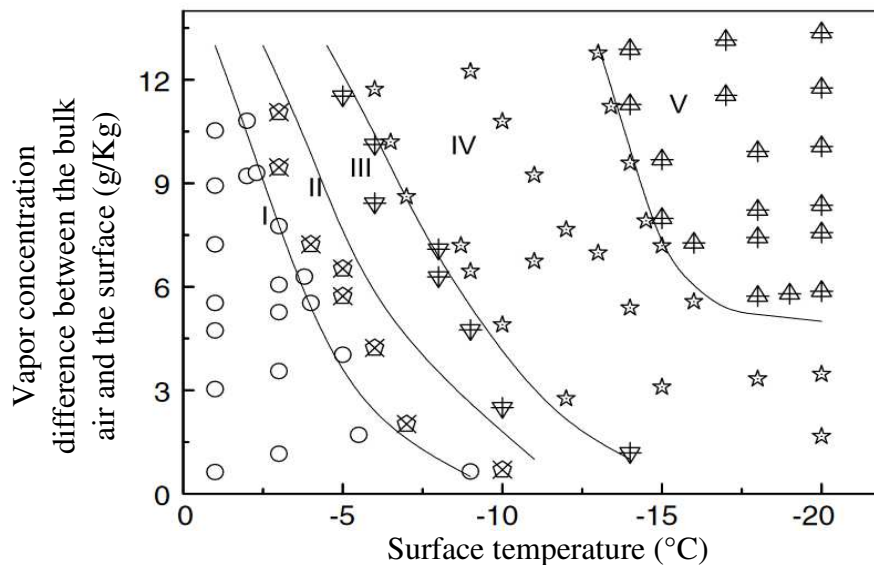


**Figure 6: Effect of surface temperature and air humidity on the shape of the earliest ice crystals; I: super-cooled water droplets, II: irregular crystals, III: flake crystals, IV: needle and pole crystals, V: feather crystals [47].**

### 3.2 Frost growth and properties

Frost growth is a complicated process because of the characteristics of frost that change depending on several environmental and technical parameters; they are also influenced by time and history during this process. Nevertheless, Hayashi et al. [53] demonstrated that the process itself, independently of

frost properties, can be considered as a common process that can be divided generally into three periods:

- Crystal growth period: at this stage, frost crystals form on the cold surface and, as they are generally distant from each other, they begin to develop vertically. This period can be considered as one-dimensional growth.
- Frost layer growth period: branches are generated around the top of the crystals so they interact with each other, forming a more uniform layer where the growth becomes more three-dimensional.
- Full growth of the frost layer: at this level, the crystals stop changing size and shape, the frost layer becomes flatter, then the surface begins to melt allowing the condensed water to diffuse inside the frost layer, thereby increasing its density. Then the deposition of frost begins again and the cycle; melting, freezing, deposition continues.

### **3.2.1 Experimental studies**

Several experimental studies have been performed to understand how frost dynamics vary the major parameters affecting frost on a heat exchanger surface; these parameters appear to be air humidity and velocity, plate temperature, the location on the heat exchanger, and the location of the heat exchanger itself. Certain experimental studies have led to the proposal of empirical relationships that can be used to predict the thickness of frost, its density and its thermal conductivity as a function of several parameters. These correlations will be discussed in the next paragraphs.

All the studies that have been conducted on flat plates [54], parallel plates and cylinders [20], microchannels [55] and finned tube heat exchangers [56], agree that the frost thickness increases as the humidity of the air increases and the temperature of the cold surface decreases. A large temperature difference between the air stream and the plate surface, and high air humidity, respectively, allow increasing of the mass transfer flow and raise the driving force of deposition, thus accelerating frost thickening. However, experimentally, the effect of air inlet velocity has revealed a considerable contradiction in the literature regarding the dependency of frost thickness on air velocity [57]. Based on experimental measurement of frost thickness on a cooled cylindrical tube at  $-25\text{ }^{\circ}\text{C}$ , Schneider [58] found that varying the air velocity from 1.2 to 10 m/s had no effect on the frost thickness. Schneider suggested a correlation to predict the frost thickness depending on time and the temperature difference between frost surface and cooled wall excluding the air velocity. In contrast, results from Hosoda et al. [8], and Barzanoni et al. [59], showed a great dependence between the frost thickness and air velocity. According to them, increasing the air velocity increases the frost thickness.

Lee and Ro [48] experimentally examined the effect of operating conditions on the growth of frost on a vertical aluminum plate. Lee and Ro found that the effect of velocity is minor compared to that of air humidity and of cooling surface temperature on frost thickness. At  $-15\text{ }^{\circ}\text{C}$  wall temperature and  $15\text{ }^{\circ}\text{C}$

air temperature, the frost thickness seems to increase slightly from 3 to 3.2 mm for Reynolds numbers ranging from 1000 to 2000, respectively.

Recently, Leoni et al. [52] made a test bench to propose new data on frost formation on a flat plate exposed to a humid airflow inside a closed-loop wind-tunnel. At -14.3 °C wall temperature, 12 °C air temperature, and an air relative humidity of 80% and by varying the air velocity from 2 m/s to 4 m/s; frost seems a little bit thicker at low air velocity. In Table 2, the three evaluations of the relationship between frost thickness and air velocity and their interpretations are grouped together.

**Table 2: Frost thickness and air velocity relationship interpretation in the literature.**

<b>Frost thickness and air velocity relationship</b>	<b>Independent</b>	<b>Proportional</b>	<b>Inversely proportional</b>
<b>Interpretation</b>	Both total and densification mass fluxes increase with velocity, thus, the mass growth flux remains constant.	A low air velocity means a small amount of vapor transferred into the frost layer from the moist air and therefore a thin frost layer.	At high air velocity, the high convective exchange coefficient heat the frost surface and thus favor the diffusion of steam inside the frost layer decreasing its thickness.

O’Neal and Tree [60] explained this contradiction by showing the existence of a critical Reynolds number of approximately 13000 above which frost growth on a flat plate is independent. This conclusion was confirmed experimentally by Lee et al [61]. The latter investigated the effect of varying the operating conditions on frost thickness and noticed that there is little difference in frost thickness if the inlet air velocity is over 2 m/s (Reynolds number > 1000).

In the same way, the variation of frost density has been analyzed experimentally by many authors. A parametric study of the literature data of a flat plate performed by Leoni et al. [57], showed that the increase of the Reynolds number causes the occurrence of a denser frost layer. When the air velocity is high, mass and heat transfer increase, leaving less space for air in the porous layer [40]. In addition, high wall temperatures favor frost densification; the mass flow that contributes to the increase in the layer mass is higher than that contributing to the increase in thickness [62].

As for humidity, its effect on frost density remains to be clarified because some disagreements continue in the literature [52]. On one hand, Hermes et al. [40] investigated experimentally the frost densification on a flat surface (100 mm × 100 mm) cooled at -15 °C by a thermoelectric cooling device including the aluminum plate on the cold side and an air source heat exchanger on the hot-side. The plate was exposed to an airflow at 22 °C that was driven by an axial fan at velocity of 0.7 m/s. Hermes et al. [40] noticed that two hours after starting the test, the frost density was 2 times higher at

an air relative humidity of 80% compared to 50%. On the other hand, frost growth experiments were conducted by Wang et al. [42] on a cold flat plate (40 mm × 40 mm) under variant frosting conditions. By maintaining constant the air temperature at 0 °C, the plate temperature at -16 °C, and the air velocity at 5 m/s; the average frost density after one hour was around 200, 250 and 220 kg/m<sup>3</sup> for air relative humidities of 42%, 53% and 72%, respectively. This means that the frost density was higher for medium relative humidity.

Lee et al. [63] performed an experimental study on the effect of air temperature, air humidity, and air velocity on frost growth on a finned-tube heat exchanger. They found that increasing the air inlet relative humidity leads to a thicker frost layer with a lower frost density and thus a higher thermal resistance. Increasing the air velocity leads to a reduction in frost thermal resistance, an increase in frost thickness, and an increase in frost density. Increasing the inlet air temperature results in a reduction of frost thickness, an increase in frost density, and a decrease of thermal resistance. It should be noted that the relative humidity was not held constant during certain tests. As a result, the conclusions of this parametric study were likely inconclusive. Recently, a series of experiments were carried out by Liping et al. [64] in order to investigate the effect of ambient conditions on the frost growth characteristics on a single row fin-tube heat exchanger. The experiments were conducted in a psychrometric room where the air temperature and relative humidity were controlled to vary between -3 °C and 0 °C and between 65% and 85%, respectively. All their results were consistent with those of Lee et al. [63]. Liping et al. [64] also added that for their cases, the effect of air inlet velocity on frost thickness was very low.

Finally, it seems difficult to decide and generalize the effect of each independent parameter on frost growth and densification. It depends on several parameters that have to be combined to precisely determine their effects.

### **3.2.2 Theoretical and numerical studies**

Theoretical and numerical studies have been also conducted to clearly understand frost growth dynamics. Three main categories of frost models exist in the literature:

*Models based on empirical correlations:* They aim at predicting frost characteristics, mainly frost thickness, density and thermal conductivity [18] over time and as a function of operating conditions. However, these models are specific to particular cases and the operating conditions used for their development. They are not always applicable in other operating conditions and different contexts. An interesting recent review [18] listed the frost layer properties (thickness, density, and thermal conductivity), heat transfer and mass transfer correlations that have been investigated since 1970. Under freezer operating conditions, and according to the author's knowledge, only one correlation developed by Mao et al. [31] has been able to predict frost properties for low wall and air temperatures, high air humidity and large air velocity intervals. Based on an experimental investigation of frost growth on a cold plate, the authors survey the frost characteristics variation over a large surface (600 mm × 200 mm) using special measurement techniques. The laser beam method

was used to measure the frost height and many removable disks flush mounted in the cold base plate permitted the measurement of frost mass concentration. Twenty tests were done for steady operating conditions; each were run for two hours. Depending on the cold plate temperature and the relative humidity of the supply air, Mao et al. [31] found that the frost could appear either smooth or rough. Depending on these two parameters, the authors suggested a map showing the frost surface characteristics. Doing this, they propose three groups of correlations. Ones for the rough frost surface, ones for the smooth surface, and more general correlations for both of them. In each correlation, frost characteristics were correlated as a function of five independent variables expressed as follow:

$$m_{fr}'' , \delta_{fr} , \rho_{fr} , k_{fr} = \alpha (x^*)^{C1} (\omega)^{C2} (T^*)^{C3} Re^{C4} F_o^{C5} \quad (1)$$

Where  $x^*$  is the ratio of the distance from the leading edge and the inlet hydraulic diameter,  $\omega$  is the inlet air humidity ratio,  $T^*$  is a cold plate temperature ratio, Re is Reynolds number, and  $F_o$  is Fourier number. These correlations are available for the operating conditions reported in Table 1 and that are typical of many industrial and commercial freezers. Table 3 summarizes the resultant correlations classified on each frost surface type.

**Table 3: Correlations of Rough and Smooth frost surface for frost properties under freezer operating conditions [31].**

Frost properties	Frost surface	Intercept and Exponents					
		$\alpha$	C1	C2	C3	C4	C5
Density $\rho_{fr}$ (kg.m <sup>-3</sup> )	Smooth	$1.334 \times 10^4$	-0.048	0.506	1.371	-0.435	0.318
	Rough	$1.601 \times 10^{-1}$	-0.056	-0.011	0.845	0.463	0.217
	Both	$0.955 \times 10^3$	-0.053	0.317	1.130	-0.279	0.328
Thickness $\delta_{fr}$ (m)	Smooth	$1.908 \times 10^{-8}$	-0.102	0.123	-2.034	1.054	0.885
	Rough	$9.183 \times 10^{-5}$	-0.085	0.400	-1.712	0.449	0.699
	Both	$1.989 \times 10^{-8}$	-0.092	0.203	-1.971	1.220	0.663
Mass concentration $m_{fr}''$ (kg.m <sup>-2</sup> )	Smooth	$2.748 \times 10^{-4}$	-0.151	0.635	-0.645	0.612	1.209
	Rough	$1.462 \times 10^{-5}$	-0.140	0.389	-0.867	0.913	0.917
	Both	$1.917 \times 10^{-5}$	-0.146	0.524	-0.836	0.943	0.993
Thermal conductivity $k_{fr}$ (W.m <sup>-1</sup> .K <sup>-1</sup> )	Smooth	$0.266 \times 10$	-0.043	0.444	1.204	-0.400	0.246
	Rough	$1.633 \times 10^{-3}$	-0.048	0.004	0.737	0.357	0.180
	Both	$0.2752 \times 10^2$	-0.046	0.283	0.984	-0.275	0.273

Computational Fluid Dynamics (CFD) based models have been developed mainly to accurately predict detailed phenomena like the frost layer structure and the distribution of absolute humidity inside the frost layer [65–69]. These models can be used to predict and simulate the macroscopic

behavior of the frost layer. Computational fluid dynamics method could be classified into three categories. The first type does not take into account the airflow side, focusing only on frost. The heat and mass transfer from the air to the frost region are then calculated using empirical correlations assuming either the humid air near to the frost surface was saturated [61,70] or supersaturated [71,72]. The second group uses models based on Eulerian multi-phase representation and they considered two phases: the primary one is gas (air side), and the secondary one is ice. Such dual phases had been widely used recently. Many researchers have successfully calculated the frost properties by solving governing equations in both sides and by using matching conditions to balance the energy and mass flows between the domains. Lee et al. [73] developed a CFD based model including partial differential equations for the boundary layer in order to consider the airflow variation. Their model was successfully validated against experimental data conducted on a cold plate at temperature of  $-15\text{ }^{\circ}\text{C}$  with laminar and turbulent flow [69,74]. Lenic et al. [75] developed a transient two-dimensional model defining governing equations of air, frost sub-domain and the air-frost interface. The developed model was validated by experimental measurements carried out on a flat plate at a temperature of  $-19.5\text{ }^{\circ}\text{C}$  and for different inlet air temperatures and relative humidity in the range  $19\text{-}23\text{ }^{\circ}\text{C}$  and  $37\text{-}60\%$ , respectively. Thereafter, numerical analyses have been performed and enabled the prediction of the exchanged heat flux degradation in a heat exchanger under the frost growth conditions [76]. Recently, a CFD based three dimensional model has been performed [77] including the fin, the two airflow passages (over and under the fin), and an inlet and outlet section in the computational region. Implementing the model in FLUENT, the numerical results show the frost distribution on a finned tube heat exchanger, the temperature distribution and the airflow pressure drop. The simulation conditions were  $-5\text{ }^{\circ}\text{C}$  as an initial wall temperature, and  $2\text{ }^{\circ}\text{C}$ ,  $80\%$  and  $1\text{ m/s}$  as air inlet temperature, relative humidity and velocity, respectively. Running 50 min, the frost appeared to be thicker and denser on the windward side of the heat exchanger and the pressure drop has practically doubled.

In contrast to these approaches, the third category uses the same Eulerian method but solves the governing equations in a single domain [78]. Kim et al. [67] used CFD to proposed a new water vapor mass transfer rate by modifying Sauter mean diameter and validated the model against experimental data of Lee et al. [73]. Compared to existing models, Kim et al. [67] have eliminated the two assumptions related to initial frost thickness and density. Cui et al. [66] proposed frosting mass transfer model based on the theory of nucleation and they focus not only on the frost behavior but also on the macroscopic description of the initial period of frost formation on a cold plate. Doing this, Cui et al. [65] improved this model by taking into consideration the influence of surface structure and they simulate the performance of finned tube heat exchanger under frost conditions.

In fact, under freezing conditions where the surface temperature is too low, the frost formed is highly porous. It means that two quantities of water vapor diffusing in the frost layer should be considered. The first one diffuse from the frost layer surface. The second one penetrates directly from the airflow through the spaces occupied by air inside the frost layer. However, as illustrated in **Figure 7**, in CFD

based model, the air volume inside the frost layer could be recognized as frost and the airflow into these spaces may be blocked. Such limitations have been reported in details by Lee et al. [79]; pointing out that CFD approach is still restricted to the analysis of these types of local phenomena. Moreover, the CFD based models requires a long time although a huge number of complex calculation is processed. Their application for large size industrial geometry is still not up to date.

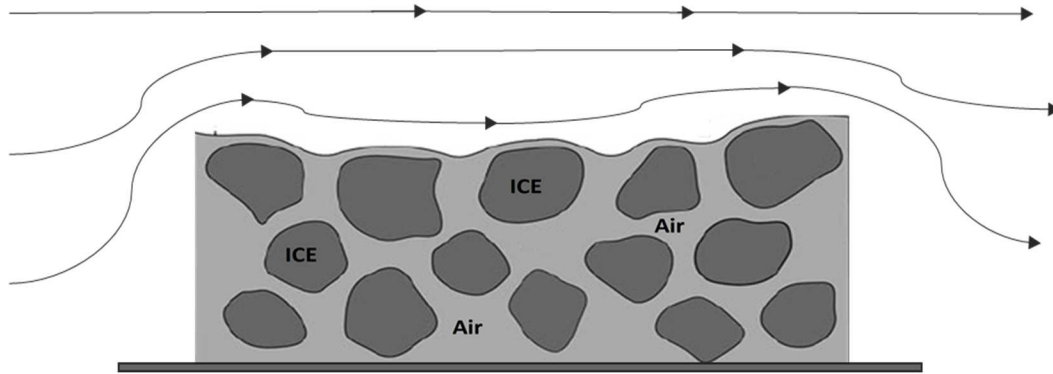


**Figure 7: Airflow in a CFD Simulation when a highly porous frost is formed, adapted from [79].**

Finally, the main approach is to develop models based on heat and mass diffusion through the frost layer considered as a porous medium [61,70,71,80,81]. These models are a good compromise between the physical phenomena taken into account and their simplicity of use for simulation. All the models based on heat and mass diffusion through the frost layer use the same set of basic equations. However, in addition to this basic set, the authors considered many different assumptions. In order to make the numerical modeling more tractable, the physical models in the literature adopt the same assumption that the water vapor transported onto the frost surface from the air stream consists of two parts. Part of this water vapor directly diffuses into the frost layer and then solidifies the frost, while the remainder deposits on the frost surface and then increases the frost thickness.

Since the frost growth period is of primary interest, especially for a system scale analysis, quasi-steady state models are more favorable and more widely used than fully transient models. Admittedly, fully transient models of frost are very interesting since they can take into account the early stage of frost formation and the spatial variation in temperature and density within the frost layer. However, fully transient models are too computationally expensive; also, the early stage of frost formation is thought to be of secondary interest, especially in a dynamic system modeling approach [23]. Figure 8 shows a diagram of all the zones and phenomena considered in the frost models. Three zones are considered: the air-stream with convective heat and mass transfer, the frost layer with heat and mass diffusion, and the interface between the two zones at the frost surface.

As explained in the previous paragraph, the overall water vapor mass flux received by the frost layer is divided into the growth and the densification mass fluxes. The water vapor mass balance can be written as:

$$\dot{m}_v'' = \frac{d}{dt}(\rho_{fr}\delta_{fr}) \quad (2)$$

$$\dot{m}_v'' = \rho_{fr} \frac{d\delta_{fr}}{dt} + \delta_{fr} \frac{d\rho_{fr}}{dt} \quad (3)$$

Where  $\delta_{fr} \frac{d\rho_{fr}}{dt} = \dot{m}_\rho''$  is the densification rate and  $\rho_{fr} \frac{d\delta_{fr}}{dt} = \dot{m}_\delta''$  is the growth rate.

The common goal of these models is to define each quantity of  $\dot{m}_\rho''$  and  $\dot{m}_\delta''$ . For this purpose, the balance equations are also defined in each zone starting from the frost-air interface going down to the cold plate. On the air-frost interface, the sensible heat transfers from the moist air to the frost surface, and the total water vapor mass flux are computed depending on the temperature gradient, and concentration gradient, respectively. Inside the frost layer, both mass and energy balances are applied to a frost element of  $dx$  thickness and the boundary conditions on the air and the wall side. The water vapor diffusion could be calculated according to Fick's law depending on effective diffusion coefficient. Heat transfer diffusion within the frost layer is then defined based on Fourier's law and finally the energy balance equations are solved defining the frost distribution temperature inside the frost layer.

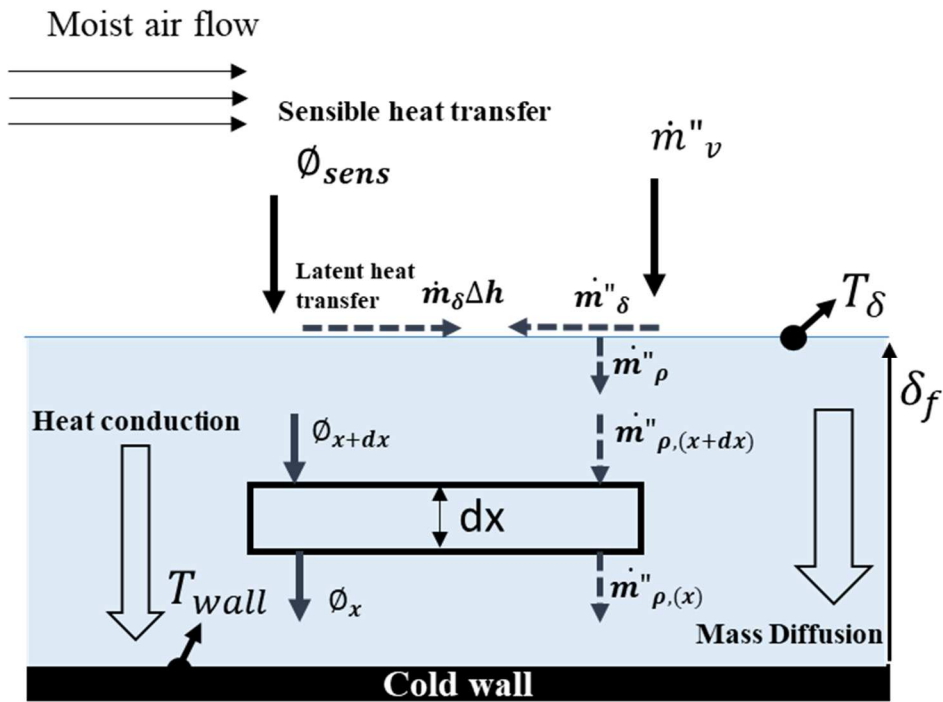


Figure 8: Transport phenomena in a porous frost layer.

Indeed, in the quasi-steady model of frost accumulation, the set of equations cannot be used without specifying different coefficients, adopting some simplifications and defining initial conditions. Therefore, frost growth is handled by different approaches regarding:

- The water vapor diffusion inside the frost layer. Either to assess the water vapor desublimation rate invariant within the frost layer [82–85], i.e. frost has a flat density profile in the perpendicular direction, so the porosity of the frost layer is uniform within the frost layer, or to consider it as proportional to the water vapor density [61,68,86];
- The water vapor saturation at the air-frost interface [62,71];
- The frost thermal conductivity. This frost property is calculated by empirical correlations proposed in the literature. Most of them correlate the thermal conductivity to the frost density but predict a large discrepancy in thermal conductivity especially for low densities;
- The initial conditions (initial frost density and thickness).

All these approaches have been analyzed and compared to experimental results by Breque and Nemer [87]. Thereafter, and through simplification, the temperature  $T_\delta$  at the surface of the frost layer can be determined analytically; also, frost thickness and density at each time step are determined. Since these models do not take into consideration the nucleation process, the equations require initial conditions of frost density and frost thickness. These conditions must be chosen carefully because they have had major impacts on many results in the literature [87]. Incidentally,  $\delta_{fr,ini} = 10^{-6} m$  and  $\rho_{fr,ini} = 30 kg/m^3$  is the most basic and common approach adopted in the literature.

Most of these modeling studies aimed to examine the effect of frost on the evaporator and not the dependence of frost growth on operating conditions. The few models used in these parametric studies have found roughly the same trends as the experimental ones described below and they have also found the same contradictions [36,88].

### 3.3 Industrial freezing specificity

When examining frosting, the main problem in an industrial freezer is to identify how much humidity is actually present inside it. In other words, it is difficult to identify the moisture sources and the humidity that they lead to. These particularities make this kind of industrial application specific in comparison to, for example, a heat pump or a simple domestic fridge.

The interest of knowing the sources of humidity in an industrial freezer is that it allows for controlling the level of undesirable humidity that can generate such frost or condensation.

The most common sources of such moisture-laden air are the products. They are considered as a major

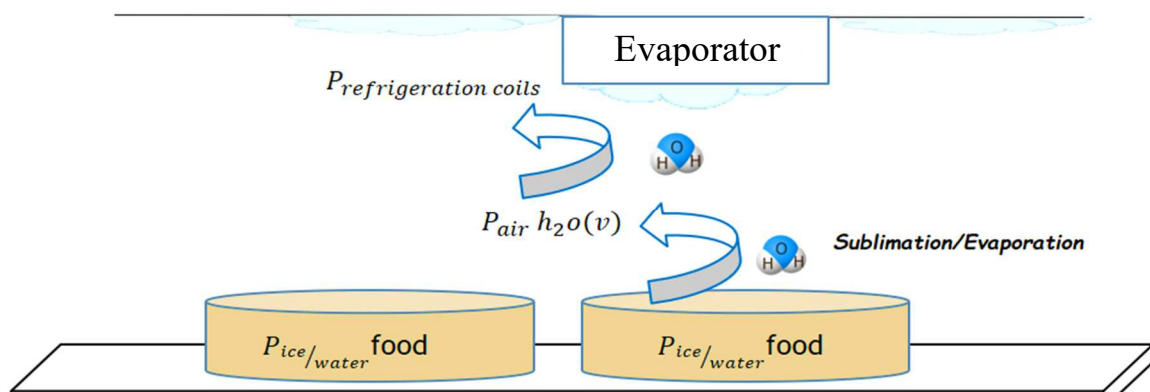


Figure 9: Illustration of mass transfer in an industrial freezer.

source of moisture when there are not packaged. In such cases, freezing induces water loss up to 6% according to the product and the freezing process [89]. The loss of water from food during the freezing process occurs because the vapor pressure of water (or ice) at the surface of food is greater than the vapor pressure of water in the air [90]. So, the water molecules migrate from the product to the coldest surface in the freezer, i.e., evaporator coils [91]. This phenomenon can be explained by the driving force expressed in terms of pressure as it can be approached in terms of temperature (Figure 9), where  $P_{\text{ice/water food}} > P_{\text{airH}_2\text{O}}(v) > P_{\text{refrigeration coils}}$ , or even  $T_{\text{ice/water food}} > T_{\text{air}} > T_{\text{refrigeration coils}}$  [92].

Product mass loss variation with time during freezing can be determined from the integral of the water vapor flux at the product surface over time [93]. The water vaporization mass flow rate (evaporation or sublimation) at the product surface ( $\dot{m}_v$ ) is expressed by:

$$\dot{m}_v = h_m A (C_{\text{vap-eq}} - C_{\text{vap-sur}}) \quad (4)$$

where  $h_m$  is the external mass transfer coefficient and  $A$  is the exchange area.  $C_{\text{vap-eq}}$  is the water vapor concentration in equilibrium with the product surface.  $C_{\text{vap-sur}}$  is the water vapor concentration in the surrounding gas (air).

Let us focus on a tunnel freezer: food products enter at a high temperature and thus a high vapor pressure at the surface, thus a large gradient will lead to mass loss. Since the freezing process is continuous, equilibrium inside will never be reached. Many authors [94,95] have highlighted other factors promoting the dehydration of frozen products such as air velocity and temperature, freezing rate and product shape (the more spherical the product, the higher the evaporation rate from its surface [96]). However, they confirmed that the difference between the pressure of water vapor or ice on the surface of the products and the surrounding air is a major cause of mass loss, which allows the vapor to escape into the air and then condense on the refrigeration coils.

Other researchers have discussed the effect of average temperature in a domestic fridge, the amplitude and frequency of temperature fluctuations on mass loss [97–99], without neglecting the effect of shape, size [100] and packaging [101], and the freezing technique [102]. All these parameters exert a great influence on the mass transfer at the solid/fluid interface which can be an important source of frost formation.

In addition, the opening of doors/barriers and pressure equalizer set-ups are also considered as major sources of moisture. Figure 10, inspired by [103], explains that in active/dynamic freezers one principal source of moisture load comes from openings as products are moved into and out of freezers. For example, in the case of an outside temperature (dock area) of 4 °C at 100 % relative humidity (RH), the partial pressure of the water vapor is 0.9135 kPa whereas it is only 0.0345 kPa inside a freezer at -30 °C at 90% RH. This pressure difference will bring the external moisture inside the freezer. This phenomenon is exacerbated when the internal temperature is lower (-40 °C) and the air infiltrating the freezer is higher. In such circumstances, the situation will become more critical.

Furthermore, the internal ventilation airflow pattern plays an important role in this disequilibrium, which makes it almost impossible to balance the pressures.

In the case of cold stores in industrial contexts, it is necessary to regularly open and close doors to move products and even if efforts are made to reduce opening times, this is not a sufficient solution. Even if the doors are always closed, air will penetrate into the store because of the negative pressure created by the temperature difference and the fans.

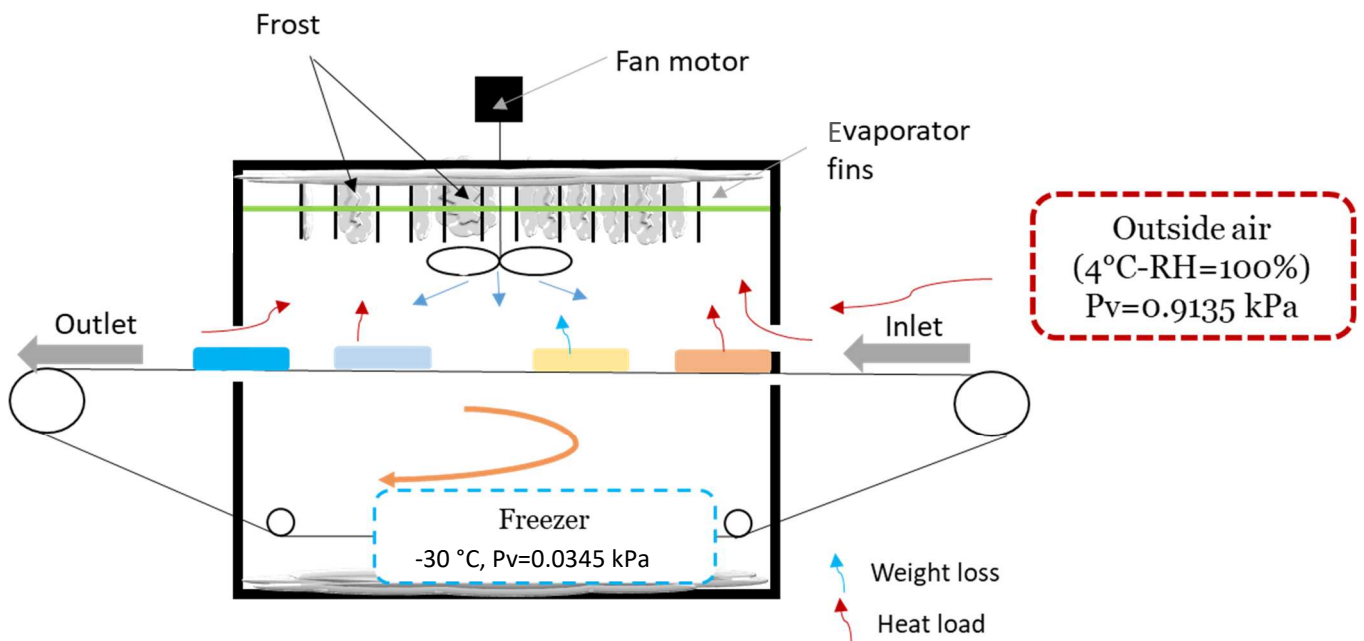


**Figure 10: Schematic of freezer air infiltration.**

The agri-food industry is always looking for more and more efficient equipment, and lately high-performance devices have been developed to increase the heat transfer coefficient between the air and the product (e.g. impingement cooler), but several technical difficulties remain to be solved [104], either to avoid frost formation or to preserve food quality.

Moreover, people entering an industrial freezing facility can also be considered as sources of humidity, especially in storage freezer, though it is relatively easy to limit these interventions to a minimum.

Finally, frost formation can be partially avoided or at least reduced by identifying humidity sources, removing the moisture at its source before entering the refrigerated space, designing sealed freezers, controlling temperature and humidity conditions. Consequently, such actions decrease unproductive interruptions, the need to defrost evaporators, and remove ice from conveyors, floors and walls.

Another specificity characterizing industrial deep freezing conditions is the occurrence of a type of frost called unfavorable frost. Indeed, frost has never been favorable for a heat exchanger but compared to another type of frost, the concept of "favorable" and "unfavorable" can be proposed. Smith, 1989-1992 [105,106] was the first to create this concept by characterizing unfavorable frost as being less dense, more insulating, and having a greater impact on coil performance.

To better understand Smith's theory, let us consider an air-cooling process. When hot air passes through a cold coil, two elementary transformations describe the overall transfer: sensible heat and latent heat transfer.

According to Figure 11, the total rate of heat transfer can be expressed by:

$$\Phi_{total} = \dot{m}_a c_a (\theta_E - \theta_S) + \dot{m}_a \Delta h (r_E - r_S) \quad (5)$$

$$\Phi_{total} = \Phi_{sens} + \Phi_{lat} \quad (6)$$

Or it can also be expressed in terms of the sensible heat load and the sensible heat ratio SHR:

$$\Phi_{total} = \frac{\Phi_{sens}}{SHR} \quad (7)$$

In general, to describe this heat transfer in a psychrometric diagram (Figure 11) a straight line connecting the conditions of the inlet air to the saturation conditions on the surface ( $\theta_{adp}$ ) is used. As a result, the slope of this line is related to the SHR ratio. Indeed, Smith's theory says that unfavorable frost occurs when this line crosses the saturation curve of the psychrometric diagram.

This situation of crossing the saturation line and then producing an unfavorable frost happens when the sensible heat coefficient SHR is too low, the humidity of the incoming air is too high, and there is a considerable temperature difference between the refrigerant and the air. This may happen in particular in industrial freezing equipment characterized by low temperature relatively confined spaces where the temperature difference between the freezer and the anteroom is greater than in the air-conditioning application. Also, the temperature of the freezer is lower than those encountered in heat pump applications [33].

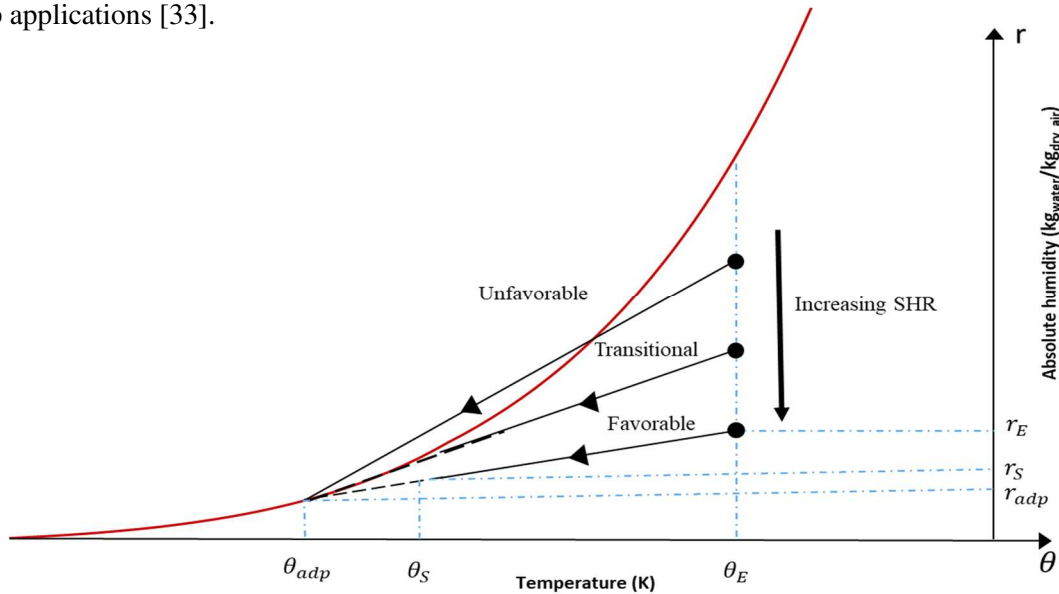


**Figure 11: Psychrometric diagram - Air heat and mass transfer through coil - favorable and unfavorable frost theory.**

Reindl and Jeckl [107] used a psychrometric chart to show a typical situation of what happens in industrial freezers when air infiltrates into a refrigerated space at a lower temperature. In Figure 12, we

differentiate three cases of an inlet air at 10°C which mixes with air from the refrigerated space at -12°C before being brought to the coil conditions represented by the apparatus dew-point temperature (ADP) at -23 °C.

- Case 1: illustrates the formation of an unfavorable frost that reflects the case of an evaporator which is located in proximity to the doors and does not give enough time to the inlet air to be mixed with the freezer air;
- Case 2: the process line is close to the saturation curve because of the small humidity value of the inlet air;
- Case 3: illustrates the formation of a favorable frost because the air entering the coil is very close to the freezer condition.

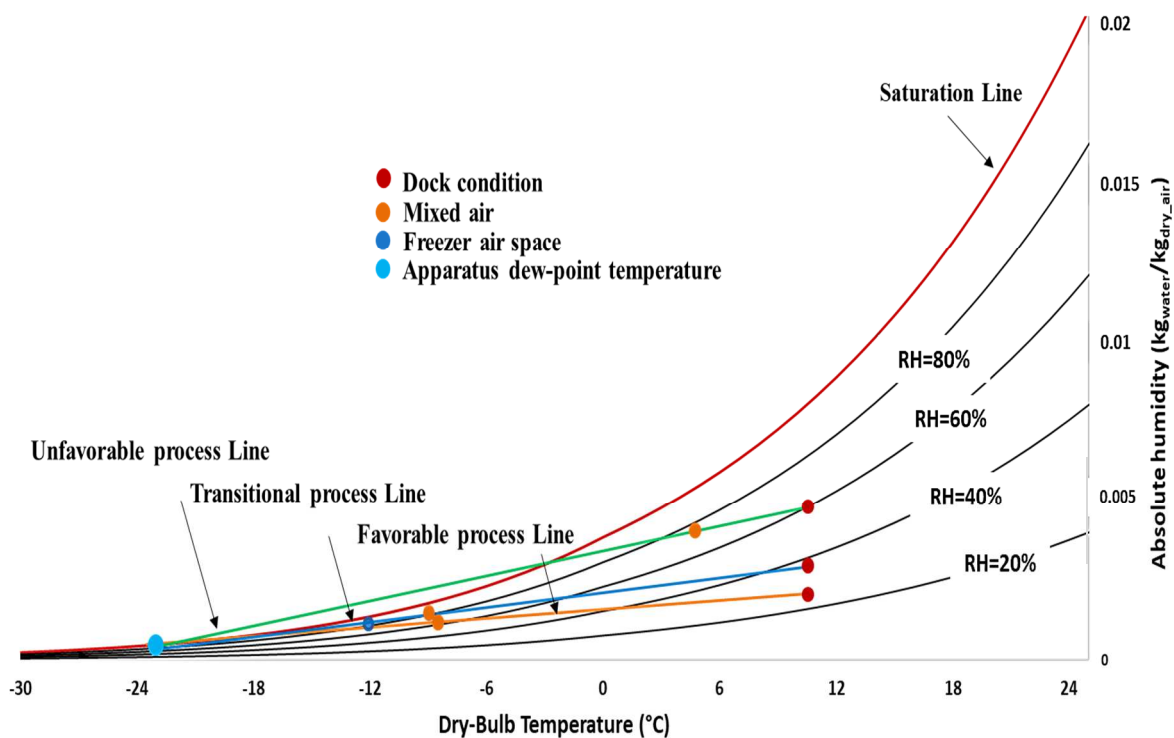


**Figure 12: Unfavorable and favorable frosting conditions on a psychrometric chart, adapted from [107].**

To validate this unfavorable and favorable frost theory, Sherif et al. [33] performed a test on a laboratory-size freezer with an industrial-size coil which was a liquid overfeed finned-tube evaporator. The experiment was performed at a cold coil temperature of -40 °C and started with a predetermined air humidity and SHR ratio, then by injecting a known amount of water vapor, the sensible heat ratio SHR decreased until the cooling process line crossed the saturation curve (Figure 11).

When the crossing occurred, the frost formation in these conditions was more a combination of two processes: a process in which ice crystals formed suspended in the air, creating airborne crystals that tended to deposit on neighboring surfaces, and a process similar to the normal (favorable) frost

formation discussed previously. In addition, the authors confirmed that unfavorable frost can be considered more insulating and less favorable from a heat transfer point of view.

#### 4. Frost Effects

Like frost growth, the frost effect has been investigated experimentally and theoretically in the literature. Several studies have been oriented towards evaluating the performance of air heat exchangers in order to understand their thermal and hydrodynamic behavior under frosting conditions. However, most of these studies only concentrated on the phenomena occurring at the heat exchanger level. The entire system behavior under frosting conditions has received relatively modest attention, especially regarding modeling.

Deng et al. [108] studied a wide range of air coolers having industrial sizes, and evaluated the overall heat transfer coefficient  $U$  and an energy transfer coefficient  $E$ , indicating the performance of heat exchangers under frosting conditions. Figure 13 shows that at an evaporation temperature of  $-10\text{ }^{\circ}\text{C}$  and an air velocity of  $3\text{ m/s}$ , an initial increase of the heat transfer coefficient occurs that can be attributed to an increase in surface roughness with the appearance of the first ice crystals, but it is still difficult to introduce this phenomenon into theoretical models. Then, as the frost continues to grow, air circulation in the air cooler is restricted and the overall heat transfer coefficient decreases. The authors also noticed that small fin spacing leads to a fast drop of the overall heat transfer and energy transfer coefficients and a rapid increase in electric power consumption. In their tests less than  $4\text{ mm}$  of frost thickness led to a  $50\%$  drop in energy performance.

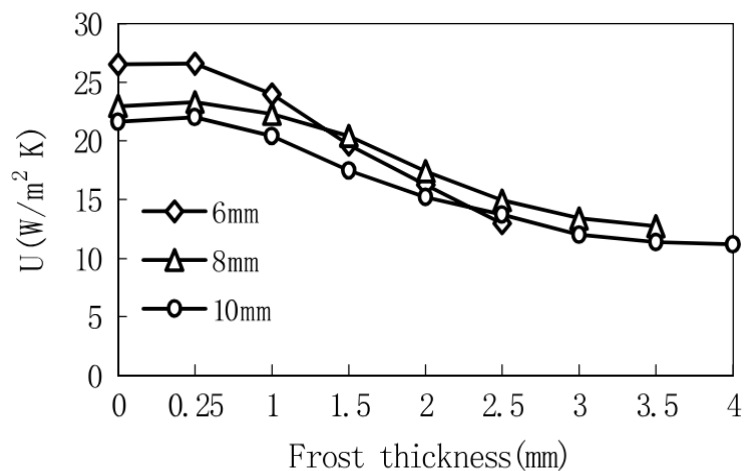


**Figure 13: Variation of overall heat transfer coefficient with frost thickness for different fin spacings ( $T_{\text{evap}}=-10\text{ }^{\circ}\text{C}$ ,  $V_a=3\text{ m/s}$ ) [108].**

An experimental and theoretical study was applied to a large-scale industrial evaporator coil as frost grew on the surfaces [38,109]. The evaporator was used to reach a space temperature of  $-29\text{ }^{\circ}\text{C}$  (evaporation temperature  $-34.4\text{ }^{\circ}\text{C}$ ). From this investigation, Aljuwayhel et al. [38,109] concluded that the mass flow rate through the evaporator coil and the evaporator cooling capacity both decreased as frost accumulated on the surface.

In 2006, Xia et al [110] evaluated the thermal-hydraulic impact of frost, defrost and refrost on five different sizes of louvered-fin, flat tube heat exchangers. They showed that in all cases frost formation induced, in two hours, a reduction of the global heat transfer coefficient and the increase of the air pressure drop, up to 50% and 80%, respectively. These authors developed a thermo-hydraulic model to estimate the performance of this type of louvered exchangers. This model has showed good agreement in terms of heat transfer coefficient but not in air pressure drop, where the discrepancies were close to 52%.

Chen et al. [31,111] developed a numerical model where the frost was treated as a transient one-dimensional porous medium. The numerical model was validated using the experimental data of a heat exchanger under frosting operating conditions. The authors showed that the effect of frost is more significant on increasing the airflow pressure drop than decreasing the heat rate exchanged. The simulations were performed for surface temperatures lower than -35 °C, air temperatures lower than -15 °C and air relative humidity up to nearly 100%. The presence of frost decreases the airflow but it also leads to its maldistribution, which can reduce the performance of the evaporator by nearly 35% [9].

Tso et al. [86] revealed that an uneven wall and air temperature distribution inside the coil of finned tube heat exchangers causes variations of the frost growth rate and densification along the coil; on the leading edge the frost thickness is greater than on the rear. In their study, a model to determine the frost distribution and dynamic behavior of an air cooler under frost conditions was developed and confirmed the previous conclusions regarding the impact of frost on heat transfer and pressure drop.

Wagner [112] conducted experimental investigations on a finned tube heat exchanger under frosting conditions and found that the airflow pressure drop across the heat exchanger is the most critical parameter influenced by frost growth. The sharp increase in pressure drop translates into an airflow decrease if this parameter is not maintained constant.

Nonetheless, most of the models available in the literature do not consider the airflow reduction that actually takes place in fan-supplied evaporator coils operating under frost conditions, which is one of the main causes of cooling capacity reduction. Most of the models were validated using experimental data collected under constant airflow conditions. One of the only studies taking into account the fan airflow reduction that occurs in real refrigerating systems due to evaporator blocking was conducted by Da Silva et al. [25]. A mathematical model was developed to analyze the influence of operational parameters on the evaporator's thermo-hydraulic performance. Experimental results collected under variable airflow conditions were used to validate the model and showed good agreement with the experimental data and also a suitable response to changes in operational conditions. It was observed that the thermal resistance due to flow blockage is the main cause for cooling capacity reduction.

Since the effects of frost accumulation are not only limited to the evaporator level, some few research have been interested by the investigation of frost on the whole system performance. These research

have shown that, under frosting conditions, the COP of a refrigeration system could be reduced by more than 15% within 40 min [52,113].

In summary, all the previous researchers agree about the harmful effects of frost accumulation. However, related researches in this area still need further elaborating in the future, primarily on the effect of frosting on energy consumption and the overall system performance.

**4.1 Industrial freezing specificity**

Following the same approach of unfavorable frost, O’Hagan [114] investigated frost formation in conditions close to those used in industry (high inlet humidity, low SHR, and high TD (air-refrigerant difference) in order to evaluate the specific thermo-hydraulic effect of this kind of frost. The authors developed a test bench which allowed them to first confirm Smith’s theory and then measure coil performance under frosting conditions. The evaluation of coil performance was done by comparing the airflow rate ( $Q_v$ ) and the sensible capacity rating ( $UA$ ) under frosting conditions with  $Q_{v,0}$  and  $UA_0$  under dry operating conditions.

Figure 14 shows several results of different SHR values taken in descending order from 0.84 to 0.54 numbered from 1 to 15. The airflow drop and coil performance degradation were greater at low SHR, which is consistent with the results observed by a number of other researchers. High relative humidity and/or a very low coil temperature (low SHR) lead to a faster decline in performance over time

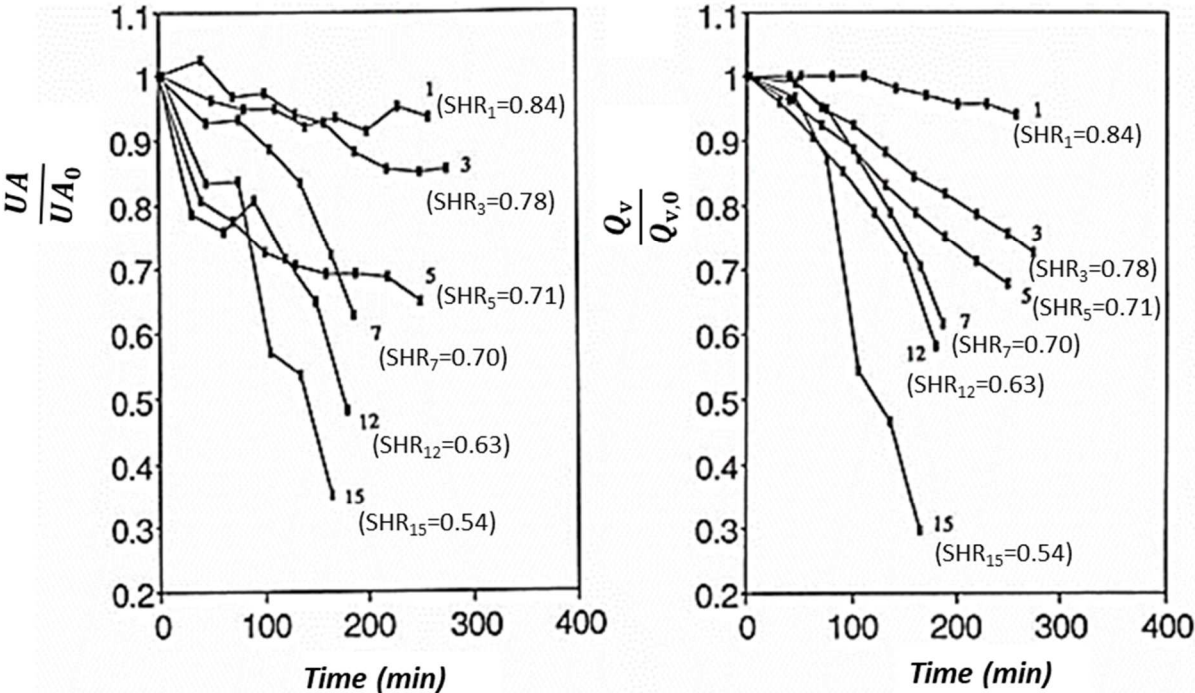


**Figure 14: Coil performance and airflow rates in frosting conditions as a function of time, adapted from [114].**

[80,115].

Furthermore, for the same amount of frost deposited, the airflow and coil performance drop were greater at low SHR, as illustrated in Figure 15. This is also consistent with Smith's theory in the fact that low SHR conditions result in less dense and less conductive frost, called "unfavorable" and which would both block the airflow and reduce heat transfer more rapidly.

In summary, and as shown in Figure 16, in industrial conditions another mechanism of frost formation in the air may appear along with frost formed classically, resulting in a less dense frost, a snow fog, thus quickly degrading the system's performance. This conclusion is consistent with Brian's study [44] discussed in section 3.1.

Moreover, the presence of frost, as explained in the frost formation mechanism in section 3.1, creates a state of non-equilibrium pressure inside the freezer, so that moisture always migrates from products to the air and then to the coldest wall in the freezer [91]. This transfer process may be responsible for cold injuries to products and quality losses.

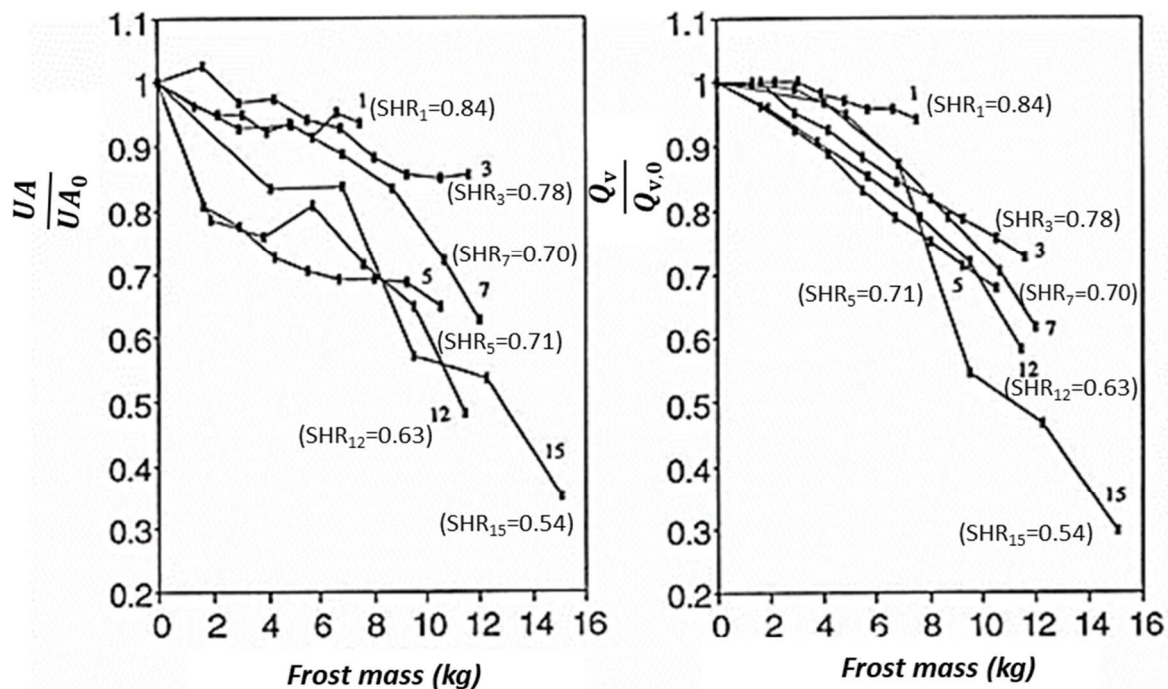


**Figure 15: Coil performance and airflow rates in frosting conditions as a function of frost mass, adapted from [114].**

In addition, frost formation often requires the freezing production line to stop for periods of defrosting which decreases the competitiveness of large continuous production lines. Furthermore, the frosting, defrosting and refrosting cycle can lead to temperature fluctuations [116,117] and to a slowdown of the production line, thereby affecting the products that will be either under or over frozen, so affecting their overall quality, texture and flavor, and ultimately the company inventory [116].

Frost on the floor and refrigerator surfaces can cause slippery surfaces dangerous for staff, while lumps of frost on the evaporator or on the roof may alter food products [118].

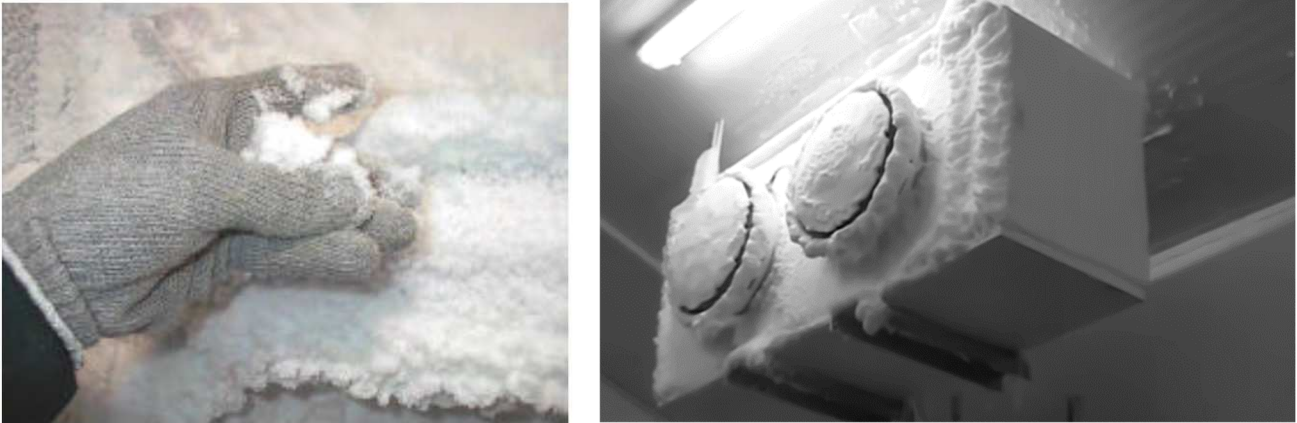


**Figure 16: Unfavorable frost forming due to the presence of supersaturated air or/and a high coil temperature difference.**

## **5. Frost management techniques**

In industry, the food cold chain must not be interrupted during the processing, packaging, storage, transport and marketing of products until they reach the final consumer. The management of this cold chain must be well planned in order to keep the food at an optimal temperature, so as to maintain its quality and ensure food safety, prevent waste and economic losses.

In the literature, many frost management techniques have been employed to tackle frost problems. We can classify these remedies into two main categories: the choice of defrosting system design, and frost formation retardation and defrosting optimization.

Recently, two reviews have been published [18,119], focusing on the development of defrosting techniques and frost retarding methods applicable for heating, ventilation, air conditioning and refrigeration systems from 1950 to 2017. Repeating the same type of literature review will not greatly contribute to the topic, which is why the purpose of this section is to place this development of frost management methods in an industrial framework. An analytical study allows meaningful conclusions to be drawn on the possibility of applying or adapting one or more of these techniques to industrial freezers characterized by low temperatures, complex geometries, large sizes and many operating constraints (e.g. continuity of production and product quality).

As for defrosting, a variety of methods are used to remove frost including compressor shutdown defrosting, thermoelectric heater defrosting, hot water spraying and hot gas defrosting [21]. However,

the most widely-used defrosting technique in industry is hot gas defrost (HGD). The HGD technique consists in using the hot gas that comes from the compressor discharge and then injecting it directly into the evaporator tubes, or by inverting the flow in the machine so the evaporator becomes a condenser, an option which is limited in the case of a single evaporator system. Few attempts in experimental or modeling studies [120,121] have been made to optimize the hot gas defrosting process either by minimizing the energy consumed during the process, or by minimizing defrosting time, energy distribution, or to predict the time and energy required to melt a frost layer. The total heat input during a hot gas process is not easily quantifiable because the hot gas is not totally condensed and the quality of the two phases leaving mixture depends significantly on the amount of frost and condensed water adhered to the coil at any instant. The energy that is extracted from the defrosting hot gas is used in many different ways: heating the evaporator coil surfaces, melting the frost, evaporating condensed water, and direct transfer to the environment. Moreover, the energy impacts associated with HGD technique depend mainly on the temperature of the refrigerant supplied for the hot gas defrost process and the defrost duration time. Higher refrigerant temperature results in short defrost periods but greater parasitic heating loads to the space. However, lower refrigerant gas temperature results in lower rate of sensible and latent gains but longer defrosting period is required to melt the accumulated frost. Because of this complexity, there have been few attempts to investigate the amount of thermal energy required for defrosting, to estimate the time required to complete defrost cycle or to understand the effect of changing some input parameters (e.g. hot gas temperature). According to Neiderer [122], only 15-20% of the total energy supplied for a typical defrosting is actually used to melt the frost. Neiderer evaluated a defrost process to remove 11.6 kg of frost from a coil over a 35 min defrosting period. For this coil, Neiderer found that 4330 kJ were used to remove the frost whereas 28043 kJ of heat was required accomplish the defrost cycle. The results of Neiderer were numerically confirmed by Hoffenbecker et al. [120]. Cole [123] notes that the energy required to melt 9.1 kg of frost from a heat exchanger weighting 669.6 kg was 4783 kJ using R22 in a hot gas bypass defrost system. In this case, 24% of the total energy supplied were used to heat the metal in the evaporator. Since this metal has a large thermal capacity and must be cooled back to the evaporator's normal operating conditions at the end of the defrosting cycle, this energy represents an additional cooling load on the freezing system.

The defrost processes of an evaporator of a cold storage freezer were analyzed by Dopazo et al. [121]. The refrigerant used is R507 and the defrost process started for an air freezer temperature measured at -15 °C, an air relative humidity at 70% and a temperature on the cold surface at -28 °C. By collecting experimental data to feed a defrost model, they obtained similar trends. The energy used to melt the accumulated frost represented 29% of the total energy supplied by the refrigerant.

On an industrial ammonia evaporator [26], it has been shown that the evaporator coil must pass through several different stages (that generally last 65 min) in order to accomplish the hot gas defrost cycle (pump-down stage, hot gas stage, bleed stage). At each stage the refrigeration system has a

specific behavior that must be included in the defrosting efficiency analysis and also in the numerical models. In general, hot gas defrost still represents a complex transient process which continue to pose further challenges in both modeling and optimization.

Surface treatment is one of the solutions that has received the most attention, and the performances of surfaces have been evaluated under frosting and defrosting conditions. Researchers have been interested in surface treatment for two reasons: to improve defrosting performance by facilitating water drainage and frost layer removal, and by delaying frost formation. Three types of surfaces have been proposed in the literature; hydrophilic, hydrophobic and slippery surfaces. These three types have shown good retardation and drainage efficiency [124]. Wang et al. [125] Reported that after 80 min of frosting, the energy consumption for defrosting were 258.8, 301.7 and 244.7 kJ for the hydrophilic, bare and hydrophobic heat exchangers, respectively. The frost layer directly detached from the hydrophobic finned tube heat exchanger at the beginning of the HGD process, thereby reducing the defrosting time by 27.2% and the mass of residual water by 48.7% compared to a bare finned tube heat exchanger. Recently, slippery surfaces have shown the excellent drainage property for the melted water during defrosting process, compared to bare, hydrophilic and hydrophobic surfaces [126]. Since these slippery surfaces are fabricated by injecting oils onto the surface structures, the oil of the surface helps to easily slide the condensed water delaying the frost formation and minimizing the defrost retained water. However, at low temperatures the efficiencies of these type of surfaces are negligible [126], [123]. Under low temperature conditions, the rate of phase change is greater than the rate of drainage and the development of drops on cold surfaces. In other words, the water vapor is rapidly transformed into ice before it can be condensed and then drained from, or slide off, the cold surface.

One well-known method in frost management is the application of an electric field. Using and increasing an electric field results in decreasing the frost growth rate, but raising the voltage to a critical point can lead to a negative effect [128]. This technique seems to be advantageous in frost delay and removal, but at low temperatures the electric field may lose this frost reduction effect.

Joppolo et al. [129] conducted several experiments measuring frost mass, air-side pressure drop and cooling capacity for different applied voltages, air velocities and evaporation temperatures on a finned-tube heat exchanger. The results showed that the electric field reduces frost mass and air-side pressure drop whereas it increases cooling capacity. Running 3 h under frosting conditions, the application of the electric field (10 kV) led to a significant energy saving about 11.5% due to the lower frost mass accumulated (lower defrosting energy consumption), lower air pressure drop (lower fan energy consumption), and higher evaporator capacity. The energy used to create the electric field has therefore a negligible effect on the overall energy consumption. As shown in Figure 17, the frost mass reduction index (MRI) is greatly reduced at low evaporation temperature. The electric field is insufficient to oppose the greater driving force of frost formation and the greater chemical potential of the phase change that results from the decrease of evaporation temperature.

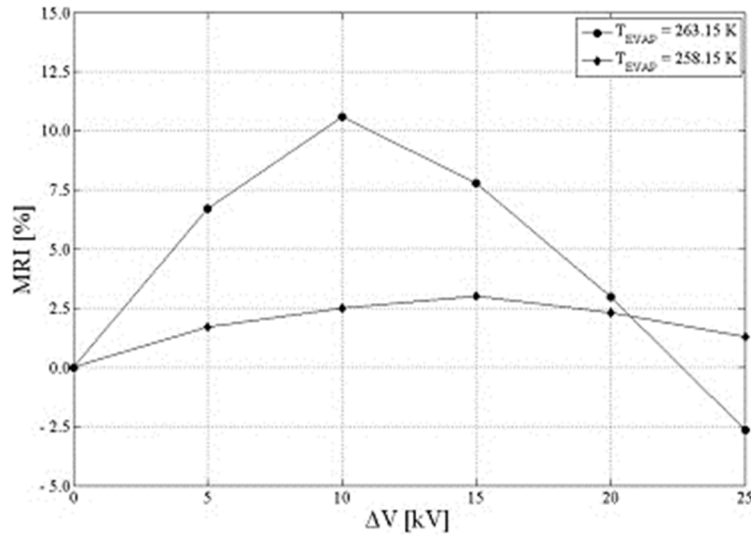


**Figure 17: Frost mass reduction versus applied voltage and evaporation temperature ( $T_a = 0\text{ }^\circ\text{C}$ ,  $RH = 80\%$ ,  $V_a = 3\text{ m/s}$ ,  $t = 10800\text{ s}$ ) [129].**

Another unusual method was proposed by Wang et al. [130]. They placed an ultrasonic vibration system on a tube-fin to eliminate frost from fins but it proved ineffective when the evaporator was fully obstructed. However, there were other limitations, in particular power consumption.

Wu et al. [16] performed frost formation experiments on several complex finned surfaces in cold surface temperatures up to  $-19\text{ }^\circ\text{C}$  and found that heat exchanger geometries had a great effect on frost layer morphology and frost distribution. Also, the influence of fin orientation showed that more frost forms on horizontal fins than on vertical ones. Xia et al. [110] conducted an impact assessment test for frosting and defrosting on louvered-fin, flat-tube heat exchangers but with different geometrical parameters. This study showed that fin depth and pitch have an effect on sequential frost-defrost cycles. The wedge formed by adjacent fins tends to retain water droplets during a defrost process. These droplets freeze during subsequent re-frosting cycles, causing a considerable effect on pressure drop and heat transfer but also on frost morphology. Lee and Kim [131] performed experimental tests of the effects of fin pitch and arrangement on heat exchanger performance under frosting conditions and found that the frost layer is thinner and denser when decreasing fin pitch. The higher air velocity of air flowing between the smaller fin spacing causes higher frost surface temperatures. Therefore, the gradients of temperature and water vapor in the frost layer become higher, and more water vapor is diffused into the frost layer. The authors proposed to determine operating conditions using the maximum allowable blockage ratio for each fin spacing. Da Silva et al. [132] also showed that the closer the fins are, the more significant the frost problem is. That means that a higher fin density leads to faster frost blocking and shorter running time [133]. It is certain that increasing the fin spacing increases the operating time but it also decreases the cooling capacity due to the small heat transfer area [63]. Confronted with this problem of maintaining both optimal normal operating and frosting-defrosting performances, Kim and Lee [134] tested three fin pitches and found that 16 FPI (fins per

inch) which is equal to 630 fins per meter showed the best thermal performance even during re-frosting cycles, compared to 14 and 18 FPI.

Furthermore, other frost management techniques were proposed via defrosting control strategies, by controlling air pressure difference, refrigerant superheat degree [135], or by measuring and detecting frost formation [136–138]. But so far, it has not been possible to generalize most of the studies performed and come up with a strong conclusion. Many proposals have been limited by the conditions in which they were tested.

### **5.1 Industrial freezing specificity**

As pointed out previously, several frost management solutions have been proposed, but few of them were tested under closed industrial conditions.

- In brief, most companies use hot gas defrost, especially in large installations, whereas electric defrosting is used mainly in small installations.
- Coating or surface treatment does not seem to be very effective at low temperatures and high humidity. Slippery surfaces had the best characteristics during frosting and defrosting but their efficiency decreases at a temperature of -10 °C and it is sure they can be adapted to a temperature as low as -40 °C. Thus, hydrophobic surfaces require further tests in industrial conditions.
- The vibration system does not allow the complete removal of frost but the most important practical limitation in the food industry is mainly the size of the evaporator and its resulting high energy consumption, not to speak of machine fatigue.
- The application of an electrical voltage seems to have a lower effect on frost formation at low temperatures than at higher ones. This aspect requires more research and effort in this field.

In the previous sections (3.1, 3.3 and 4.1), an exclusive frost formation mechanism and consequently a specific type of less dense and more unfavorable frost was determined as a particularity that can occur in industrial freezers. Regarding this, O'Hagan [114] proposed two solutions; if the operation is expected to be very long under low SHR conditions, an evaporator design with large or variable fin spacing must be provided to reduce defrost frequency; and if these low SHR conditions occur only for short periods, the performance drop should not be a concern because it is recovered later.

If product moisture loss is foreseeable at the beginning of the freezing process followed by a decrease in loss-rate during the cooling cycle, the industrial company must choose the optimal defrost timing in the middle of the cycle when moving from a low SHR to a higher one, to prevent the machine from operating for a long time with low performance.

Since product moisture loss is considered as a major source of water vapor in industrial freezers, its control is of the greatest practical interest. At the freezer inlet, the food surface has a higher temperature than the circulating air, thus the surface water vapor pressure is also higher than that of the air. This difference between the water vapor pressure on the food surface and that in the surrounding atmosphere is the driving force for dehydration and it is greater as the product is initially at a higher temperature. In Figure 18, it can be seen that precooling the products from 40 °C to 20 °C before being introduced inside a freezer at -40 °C can reduce the driving force of evaporation by more than 60% when assuming the product water activity  $A_w$  is equal to 0.9. Therefore, product pre-cooling could be considered among the solutions which limit the phenomenon of water migration.

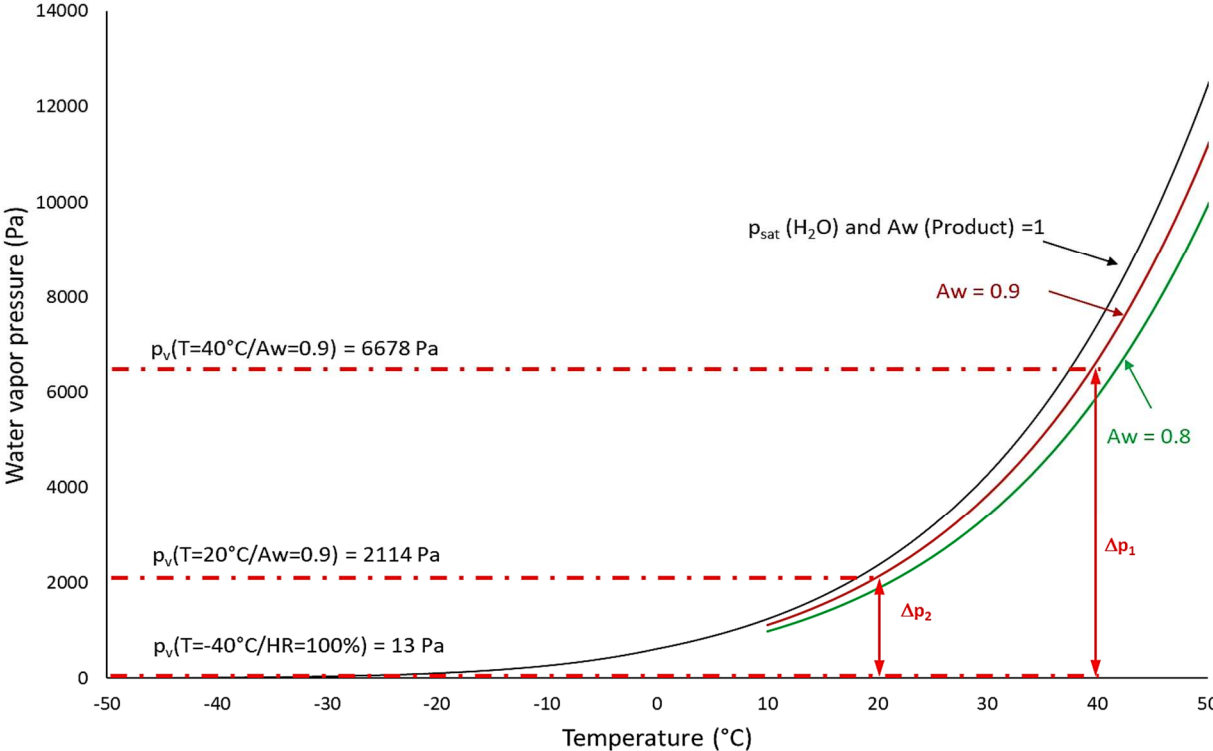


**Figure 18: Dehydration losses during freezing versus the inlet product temperature.**

Cleland [139] also proposed practical solutions for industry: the evaporator should be logically placed and installed away from doors so that the inlet air has time to mix with the air from the freezer. The author determined that it is difficult to avoid unfavorable frost formation and it is always preferable to have a larger fin spacing to avoid production dead time. In contrast, Chen [140] showed that this solution of large fin spacing causes an overconsumption of 25% which must not be overlooked in an industrial site. A critical SHR can also be determined based on an inlet air temperature or surface temperature to select the right parameters against unfavorable frost.

Another alternative that could be adopted is air inlet and dock area dehumidification [141–144] but this is still limited regarding its price. Physical solutions are also adopted by industry such as the use of curtains at the entry / exit of the freezer to limit air infiltrations, but they have not demonstrated great efficiency in limiting this effect. In addition, they may also constitute an obstacle that limits

product movements and possible hygiene problems may occur when there is direct contact between the curtains and products. Moreover, air curtains were also tested and gave satisfactory results only when the pressure imbalance was low [145].

## **6. Conclusion**

Despite the improvements made to refrigeration, freezing and deep-freezing systems, depending on the temperature and hygrometry of the air outside or inside, respectively, frosting may occur when moist air comes into contact with a cold surface whose temperature is below dew point. This frost has a negative effect on the installation energy performance but also possibly on the quality of the products frozen.

This review has covered all the aspects related to this phenomenon by placing it in the context of industrial freezing conditions, since the agri-food industry is characterized in particular by many constraints, specificities and technical difficulties and the possible emergence of other challenges that have to be solved. Based on the reported papers, the following conclusions are made:

- (1) First of all, in addition to the two traditional mechanisms of the condensation cycle of the water vapor contained in the air, then freezing or direct desublimation, industrial freezing conditions can lead to a third frost formation mechanism. Ice crystals may be formed in the air before being deposited on the evaporator and freezer surfaces. The kind of frost layer formed in these conditions of very low temperature and medium to high humidity is less dense and more unfavorable compared to the frost formed in refrigeration or heat pump applications.
- (2) To determine how frost can influence a heat exchanger's behavior, it is first necessary to determine its key characteristics: thickness, mass, density, morphology, and its distribution on the evaporator. These parameters are still difficult to manage or to estimate because the frost layer is always evolving in time, and it is complicated to determine the nature of frost since several of heat and mass diffusion phenomena come into play, especially in the frost growth phase. All these parameters vary depending on the environmental, technical and operational conditions.
- (3) While research has shown great progress, significant challenges remain associated with accurately predicting frosting and defrosting processes under wide ranges of conditions. The equations governing such behavior still remain insoluble by analytical methods. However, numerical approaches have given the most promising results, but they do not yet cover all the physical and technical aspects of a real system.
- (4) The determination of frost characteristics allows estimating the effect of frost growth on heat exchanger performance. In summary, frost on the evaporator reduces cooling capacity by increasing the air pressure drop, reducing airflow rates through the evaporator, and reducing heat transfer since the frost layer acts as an insulator.
- (5) Most of the models available in the literature were developed at a very small scale to obtain deeper understanding of the frost growth process. On a larger scale, models allow

investigation of the frosting process on an evaporator. Nonetheless, most of these models do not consider the reduction of airflow that actually takes place in fan-supplied evaporator coils operating under frost conditions, which is one of the major causes of cooling capacity reduction. Moreover, it is also necessary to develop a model based on a systemic approach to understand the behavior of each component of the freezing system under frosting conditions and to quantify the effects of frost at this global scale. Such a predictive model would permit analyzing different solutions and controlling frost development while conforming to industrial constraints of productivity and quality.

- (6) To optimize cooling systems working under frosting conditions, several strategies have been suggested to prevent the formation of frost or to eliminate frost after its formation but few solutions can be generalized or adapted to the different conditions. Very low temperatures and large installations still present challenges regarding this problem of frost management in the agri-food industry.
- (7) It is obviously recommended to limit as much as possible the sources of humidity that can occur in an industrial freezer. These sources are product moisture losses, freezer doors, openings and infiltrations. Air curtains and pressure equilibrium systems may be used to limit infiltrations. The products should preferably be precooled before being introduced in the freezer.
- (8) A frost delay strategy must be effective at low temperatures and must not lose this efficiency after several frosting-defrosting cycles. To achieve this, the hydrophobic surface seems to be of great interest for future research but no general conclusion can be drawn because of the great diversity of experimental conditions in the literature.
- (9) Defrosting sequences should be less frequent to avoid production stoppages. They must be as short as possible, not consume much energy and not allow a large transfer of moisture or heat inside the freezer. Although there is no general method or strategy for any condition, the control of defrost sequences nonetheless definitely plays an important role in quantifying the efficiency of a defrosting system.
- (10) Evaporator geometry adjustment was also shown to have a considerable effect on the amount and occurrence of frost and it is considered one of the principle optimization strategies recommended. However, this solution can only be adopted during the first phase of design. On an industrial scale especially, it is always complicated to carry out this kind of intervention later.
- (11) Numerical modeling is highly recommended for the investigation of this type of application for which experiments are more complicated. A dynamic model based on a systemic approach may be the best tool for optimization. This optimization may be defined by setting different objectives which could be either productivity objectives or energetic optimization objectives, among others.

- (12) Further academic efforts are needed to propose experimental test benches and improve measurement techniques of frost properties in order to satisfy as close as possible the industrial freezing conditions. These experimental investigations may help to generate more local data on the dynamic of frost in these specific conditions that are lacking in the literature.

According to this review, we conclude that several efforts have been made to overcome this problem of frost management. Most of the studies showed satisfactory results. However, they are still limited to a specific range of applications and they propose some technologies that are impractical in cold conditions.

Finally, the food industry is always looking for refrigeration systems that are more efficient economically and energetically but that are also adapted to its technical difficulties and operating conditions, hence the need for advanced experimental works and numerical models.

### **Acknowledgements**

The authors would like to express their gratitude for the financial support provided by the French Environment and Energy Management Agency (ADEME)

### **References**

- [1] Coulomb D. Refrigeration and cold chain serving the global food industry and creating a better future: two key IIR challenges for improved health and environment. *Trends Food Sci Technol* 2008;19:413–7. <https://doi.org/10.1016/j.tifs.2008.03.006>.
- [2] Vermeulen SJ, Campbell BM, Ingram JSI. Climate Change and Food Systems. *Annu Rev Environ Resour* 2012;37:195–222. <https://doi.org/10.1146/annurev-environ-020411-130608>.
- [3] Sutariya SG, Sunkesula V. Food Freezing: Emerging Techniques for Improving Quality and Process Efficiency a Comprehensive Review. *Innov. Food Process. Technol.*, Elsevier; 2021, p. 36–63. <https://doi.org/10.1016/b978-0-08-100596-5.23035-7>.
- [4] Sadot M, Curet S, Chevallier S, Le-Bail A, Rouaud O, Havet M. Microwave assisted freezing part 2: Impact of microwave energy and duty cycle on ice crystal size distribution. *Innov Food Sci Emerg Technol* 2020;62:102359. <https://doi.org/10.1016/j.ifset.2020.102359>.
- [5] Schudel S, Prawiranto K, Defraeye T. Comparison of freezing and convective dehydrofreezing of vegetables for reducing cell damage. *J Food Eng* 2021;293:110376. <https://doi.org/10.1016/j.jfoodeng.2020.110376>.
- [6] Bøgh-Sørensen L. Recommendations for the Processing and Handling of Frozen Foods. IFF-IIR; 2006.
- [7] Marinyuk BT. Heat and mass transfer under frosting conditions. *Int J Refrig* 1980;3:366–8. [https://doi.org/10.1016/0140-7007\(80\)90128-0](https://doi.org/10.1016/0140-7007(80)90128-0).

- [8] Hosoda T, Uzuhahi, H. Effects of Frost on the Heat Transfer Coefficient. *Hitachi Review* 1967;49:647–51.
- [9] Aganda AA, Coney JER, Sheppard CGW. Airflow maldistribution and the performance of a packaged air conditioning unit evaporator. *Appl Therm Eng* 2000;20:515–28. [https://doi.org/10.1016/S1359-4311\(99\)00038-1](https://doi.org/10.1016/S1359-4311(99)00038-1).
- [10] Sanders CT. Frost formation: The influence of frost formation and defrosting on the performance of air coolers. Faculty of Mechanical, Maritime and Materials Engineering; 1974 (Thesis).
- [11] Guo X-M, Chen Y-G, Wang W-H, Chen C-Z. Experimental study on frost growth and dynamic performance of air source heat pump system. *Appl Therm Eng* 2008;28:2267–78. <https://doi.org/10.1016/j.applthermaleng.2008.01.007>.
- [12] Heim M. Etude du givrage et du degivrage d'évaporateurs de chambre froide - Optimisation expérimentale : Institut National des Sciences appliquées, Laboratoire d'Energetique et Automatique;1989. Technical Report : DEA Transferts Thermiques.
- [13] Amer M, Wang CC. Review of defrosting methods. *Renew Sustain Energy Rev* 2017;73:53–74. <https://doi.org/10.1016/j.rser.2017.01.120>.
- [14] Mader G, Thybo C. A new method of defrosting evaporator coils. *Appl Therm Eng* 2012;39:78–85. <https://doi.org/10.1016/j.applthermaleng.2012.01.033>.
- [15] Ma Q, Wu X, Chu F, Zhu B. Experimental and numerical investigations of frost formation on wavy plates. *Appl Therm Eng* 2018;138:627–32. <https://doi.org/10.1016/J.APPLTHERMALENG.2018.04.098>.
- [16] Wu X, Hu S, Chu F. Experimental study of frost formation on cold surfaces with various fin layouts. *Appl Therm Eng* 2016;95:95–105. <https://doi.org/10.1016/J.APPLTHERMALENG.2015.11.045>.
- [17] Piucco RO, Hermes CJL, Melo C, Barbosa JR. A study of frost nucleation on flat surfaces. *Exp Therm Fluid Sci* 2008;32:1710–5. <https://doi.org/10.1016/J.EXPTHERMFLUSCI.2008.06.004>.
- [18] Song M, Dang C. Review on the measurement and calculation of frost characteristics. *Int J Heat Mass Transf* 2018;124:586–614. <https://doi.org/10.1016/j.ijheatmasstransfer.2018.03.094>.
- [19] Wang F, Liang C, Zhang X. Research of anti-frosting technology in refrigeration and air conditioning fields: A review. *Renew Sustain Energy Rev* 2018;81:707–22. <https://doi.org/10.1016/j.rser.2017.08.046>.
- [20] O'Neal DL, Tree DR. A review of frost formation in simple geometries. *ASHRAE Trans*

1985:267–81.

- [21] Song M, Deng S, Dang C, Mao N, Wang Z. Review on improvement for air source heat pump units during frosting and defrosting. *Appl Energy* 2018;211:1150–70.  
<https://doi.org/10.1016/j.apenergy.2017.12.022>.
- [22] Janssen D. Experimental strategies for frost analysis. University of Minnesota. Department of Mechanical Engineering. Minnesota; 2013 (Thesis).
- [23] Qiao H, Radermacher R. Transient modeling of two-stage and variable refrigerant flow vapor compression systems with frosting and defrosting. University of Maryland. Department of Mechanical Engineering. Maryland; 2014 (Thesis).
- [24] Zhang L, Jiang Y, Dong J, Yao Y, Deng S. A comparative study of frosting behavior on finned tube heat exchanger under different fan control modes. *Appl Therm Eng* 2019;160:114063.  
<https://doi.org/10.1016/J.APPLTHERMALENG.2019.114063>.
- [25] Da Silva DL, Hermes CJL, Melo C. First-principles modeling of frost accumulation on fan-supplied tube-fin evaporators. *Appl Therm Eng* 2011;31:2616–21.  
<https://doi.org/10.1016/j.applthermaleng.2011.04.029>.
- [26] Aljuwayhel NF. Numerical and Experimental Study of the Influence of Frost Formation and Defrosting on the Performance of Industrial Evaporator Coils. University of Wisconsin-Madison; 2006 (Thesis).
- [27] Badri D, Toublanc C, Rouaud O, Havet M. Dynamic modeling and simulation of frost formation on blast freezer heat exchanger. Proceedings of the 6th IIR Int Conf Sustain Cold Chain; 2020 August 26-28; France, Nantes;2020.  
<https://doi.org/10.18462/IIR.ICCC.2020.297099>.
- [28] Lotz H. Heat and mass transfer and pressure drop in frosting finned coils. *Refrig. Sci. Technol. Proceedings of the 12th Int. Congr. Refrig.*, 1967, p. 449–505.
- [29] Patin A. Optimisation des degivrages par gaz chauds en chambre a basse temperature. *Int J Refrig* 1990;13:325–9. [https://doi.org/10.1016/0140-7007\(90\)90064-4](https://doi.org/10.1016/0140-7007(90)90064-4).
- [30] Chen H, Thomas L, Besant RW. Modeling frost characteristics on heat exchanger fins: Part II. Model Validation and Limitations. *ASHRAE Trans* 2000;106:368–76.
- [31] Mao Y, Chen H, Besant RW. Frost characteristics and heat transfer on a flat plate under freezer operating conditions: Part I, Experimentation and Correlations. *ASHRAE Trans* 1999;105.
- [32] Chen H, Thomas L, Besant RW. Modeling frost characteristics on heat exchanger fins: Part I. Numerical model. *ASHRAE Trans* 2000;106:357–67.

- [33] Sherif SA, Mago PJ, Al-Mutawa NK, Theen RS, Bilen K, Besant RW. Psychrometrics in the supersaturated frost zone. *ASHRAE Trans* 2001;107 PART 2:753–67.
- [34] Verma P, Bullard CW, Hrnjak PS. Design Tool for Display Case Heat Exchanger Frosting and Defrosting : Air Conditioning and Refrigeration Center; 2002. Technical Report No: TR-201.
- [35] Aljuwayhel NF, Reindl DT, Klein SA, Nellis GF. Experimental investigation of the performance of industrial evaporator coils operating under frosting conditions. *Int J Refrig* 2008;31:98–106. <https://doi.org/10.1016/j.ijrefrig.2007.05.010>.
- [36] Seker D, Karatas H, Egrican N. Frost formation on fin-and-tube heat exchangers. Part I - Modeling of frost formation on fin-and-tube heat exchangers. *Int J Refrig* 2004;27:367–74. <https://doi.org/10.1016/j.ijrefrig.2003.12.003>.
- [37] Seker D, Karatas H, Egrican N. Frost formation on fin-and-tube heat exchangers. Part II - Experimental investigation of frost formation on fin-and-tube heat exchangers. *Int J Refrig* 2004;27:375–7. <https://doi.org/10.1016/j.ijrefrig.2003.12.004>.
- [38] Aljuwayhel NF, Reindl DT, Klein SA, Nellis GF. Comparison of parallel- and counter-flow circuiting in an industrial evaporator under frosting conditions. *Int J Refrig* 2007;30:1347–57. <https://doi.org/10.1016/J.IJREFRIG.2007.04.009>.
- [39] Piucco RO, Hermes CJL, Melo C, Barbosa JR. A study of frost nucleation on flat surfaces. *Exp Therm Fluid Sci* 2008;32:1710–5. <https://doi.org/10.1016/J.EXPTHERMFLUSCI.2008.06.004>.
- [40] Hermes CJL, Piucco RO, Barbosa JR, Melo C. A study of frost growth and densification on flat surfaces. *Exp Therm Fluid Sci* 2009;33:371–9. <https://doi.org/10.1016/J.EXPTHERMFLUSCI.2008.10.006>.
- [41] Cao Z, Han H, Gu B, Ren N. A novel prediction model of frost growth on cold surface based on support vector machine. *Appl Therm Eng* 2009;29:2320–6. <https://doi.org/10.1016/j.applthermaleng.2008.11.015>.
- [42] Wang W, Guo QC, Lu WP, Feng YC, Na W. A generalized simple model for predicting frost growth on cold flat plate. *Int. J. Refrig.*, vol. 35, Elsevier; 2012, p. 475–86. <https://doi.org/10.1016/j.ijrefrig.2011.10.011>.
- [43] Kumala EF, Priramadhi RA, Pangaribuan P. Frost Preventive Control System of Freezer. *Proceedings of IOP Conf. Ser. Mater. Sci. Eng.*, vol. 434, Institute of Physics Publishing; 2018. <https://doi.org/10.1088/1757-899X/434/1/012216>.
- [44] Brian PLT, Reid RC, Shah YT. Frost Deposition on Cold Surfaces. *Ind Eng Chem Fundam* 1970;9:375–80. <https://doi.org/10.1021/i160035a013>.

- [45] Kobayashi T. On the Habit of Snow Crystals Artificially Produced at Low Pressures. *J Meteorol Soc Japan Ser II* 1958;36:193–208. [https://doi.org/10.2151/jmsj1923.36.5\\_193](https://doi.org/10.2151/jmsj1923.36.5_193).
- [46] Qu K, Komori S, Jiang Y. Local variation of frost layer thickness and morphology. *Int J Therm Sci* 2006;45:116–23. <https://doi.org/10.1016/J.IJTHEMALSCI.2005.05.004>.
- [47] Wu X, Dai W, Xu W, Tang L. Mesoscale investigation of frost formation on a cold surface. *Exp Therm Fluid Sci* 2007;31:1043–8. <https://doi.org/10.1016/j.expthermflusci.2006.11.002>.
- [48] Lee Y., Ro S. Frost formation on a vertical plate in simultaneously developing flow. *Exp Therm Fluid Sci* 2002;26:939–45. [https://doi.org/10.1016/S0894-1777\(02\)00216-9](https://doi.org/10.1016/S0894-1777(02)00216-9).
- [49] Tajima O, Yamada H, Kobayashi LM. Frost Formation on Air Coolers, Part I: Natural Convection for a Flat Plate Facing Upwards. *Heat Tans Japanese Res* 1972;1:39–48.
- [50] Cremers CJ, Mehra VK. Frost Formation on Vertical Cylinders in Free Convection. *J Heat Transfer* 1982;104:3. <https://doi.org/10.1115/1.3245065>.
- [51] Han H, Ro ST. The characteristics of frost growth on parallel plates. In : Hutter K, Wang Y, Beer H, eds. *Advances in Cold-Region Therm. Eng. Sci.*, Springer Berlin Heidelberg;1999, p. 55–64.  
<https://doi.org/10.1007/BFb0104171>.
- [52] Leoni A. Etude Experimentale et modelisation de la formation et du developpement du givre sur une plaque refroidie. CETHIL, Lyon University; 2017 (Thesis).
- [53] Hayashi Y, Aoki A, Adachi S, Hori K. Study of frost properties correlating with frost formation types. *J Heat Transfer* 1977;99:239–45. <https://doi.org/10.1115/1.3450675>.
- [54] Leoni A, Mondot M, Durier F, Revellin R, Haberschill P. Frost formation and development on flat plate: Experimental investigation and comparison to predictive methods. *Exp Therm Fluid Sci* 2017;88:220–33. <https://doi.org/10.1016/j.expthermflusci.2017.06.005>.
- [55] Moallem E, Cremaschi L, Fisher DE, Padhmanabhan S. Experimental measurements of the surface coating and water retention effects on frosting performance of microchannel heat exchangers for heat pump systems. *Exp Therm Fluid Sci* 2012;39:176–88.  
<https://doi.org/10.1016/j.expthermflusci.2012.01.022>.
- [56] Amini M, Pischevar AR, Yaghoubi M. Experimental study of frost formation on a fin-and-tube heat exchanger by natural convection. *Int J Refrig* 2014;46:37–49.  
<https://doi.org/10.1016/J.IJREFRIG.2014.06.015>.
- [57] Léoni A, Mondot M, Durier F, Revellin R, Haberschill P. State-of-the-art review of frost deposition on flat surfaces. *Int J Refrig* 2016;68:198–217.

- <https://doi.org/10.1016/j.ijrefrig.2016.04.004>.
- [58] Schneider HW. Equation of the growth forming on cooled surfaces. *Int J Heat Mass Transf* 1978;21:1019–24. [https://doi.org/10.1016/0017-9310\(78\)90098-4](https://doi.org/10.1016/0017-9310(78)90098-4).
- [59] Barzanoni Y, Noorshams O, Tabrizi HB, Damangir E. Experimental investigation of frost formation on a horizontal cold cylinder under cross flow. *Int J Refrig* 2011;34:1174–80. <https://doi.org/10.1016/j.ijrefrig.2011.02.011>.
- [60] O’Neal DL, Tree DR. Measurement of frost growth and density in a parallel plate geometry. *ASHRAE Trans* 1984;90:278–90.
- [61] Lee K-S, Kim W-S, Lee T-H. A one-dimensional model for frost formation on a cold flat surface. *Int J Heat Mass Transf* 1997;40:4359–65. [https://doi.org/10.1016/S0017-9310\(97\)00074-4](https://doi.org/10.1016/S0017-9310(97)00074-4).
- [62] El Cheikh A, Jacobi A. A mathematical model for frost growth and densification on flat surfaces. *Int J Heat Mass Transf* 2014;77:604–11. <https://doi.org/10.1016/j.ijheatmasstransfer.2014.05.054>.
- [63] Lee TH, Lee KS, Kim WS. The Effects of Frost Formation in a Flat Plate Finned-Tube Heat Exchanger. *Proceedings of Int. Refrig. Air Cond. Conf* 1996;205-210.
- [64] Liping X, Xianmin G, Zhen X. Experimental Study of Frost Growth Characteristics on Surface of Fin-tube Heat Exchanger. *Energy Procedia* 2017;105:5114–21. <https://doi.org/10.1016/J.EGYPRO.2017.03.1039>.
- [65] Cui J, Li WZ, Liu Y, Zhao YS. A new model for predicting performance of fin-and-tube heat exchanger under frost condition. *Int J Heat Fluid Flow* 2011;32:249–60. <https://doi.org/10.1016/j.ijheatfluidflow.2010.11.004>.
- [66] Cui J, Li WZ, Liu Y, Jiang ZY. A new time- and space-dependent model for predicting frost formation. *Appl Therm Eng* 2011;31:447–57. <https://doi.org/10.1016/j.applthermaleng.2010.09.022>.
- [67] Kim D, Kim C, Lee KS. Frosting model for predicting macroscopic and local frost behaviors on a cold plate. *Int J Heat Mass Transf* 2015;82:135–42. <https://doi.org/10.1016/j.ijheatmasstransfer.2014.11.048>.
- [68] Kim JS, Lee KS, Yook SJ. Frost behavior on a fin considering the heat conduction of heat exchanger fins. *Int J Heat Mass Transf* 2009;52:2581–8. <https://doi.org/10.1016/j.ijheatmasstransfer.2008.12.023>.
- [69] Yang DK, Lee KS, Cha DJ. Frost formation on a cold surface under turbulent flow. *Int J Refrig*

- 2006;29:164–9. <https://doi.org/10.1016/j.ijrefrig.2005.07.003>.
- [70] Jones BW, Parker JD. Frost formation with varying environmental parameters. *J Heat Transfer* 1975;97:255–9. <https://doi.org/10.1115/1.3450350>.
- [71] Na B, Webb RL. New model for frost growth rate. *Int J Heat Mass Transf* 2004;47:925–36. <https://doi.org/10.1016/j.ijheatmasstransfer.2003.09.001>.
- [72] Na B, Webb RL. Mass transfer on and within a frost layer. *Int J Heat Mass Transf* 2004;47:899–911. <https://doi.org/10.1016/j.ijheatmasstransfer.2003.08.023>.
- [73] Lee KS, Jhee S, Yang DK. Prediction of the frost formation on a cold flat surface. *Int J Heat Mass Transf* 2003;46:3789–96. [https://doi.org/10.1016/S0017-9310\(03\)00195-9](https://doi.org/10.1016/S0017-9310(03)00195-9).
- [74] Yang DK, Lee KS. Modeling of frosting behavior on a cold plate. *Int. J. Refrig.*, vol. 28, 2005, p. 396–402. <https://doi.org/10.1016/j.ijrefrig.2004.08.001>.
- [75] Lenic K, Trp A, Frankovic B. Transient two-dimensional model of frost formation on a fin-and-tube heat exchanger. *Int J Heat Mass Transf* 2009;52:22–32. <https://doi.org/10.1016/j.ijheatmasstransfer.2008.06.005>.
- [76] Lenic K, Trp A, Frankovic B. Prediction of an effective cooling output of the fin-and-tube heat exchanger under frosting conditions. *Appl Therm Eng* 2009;29:2534–43. <https://doi.org/10.1016/j.applthermaleng.2008.12.030>.
- [77] Wu X, Ma Q, Chu F. Numerical simulation of frosting on fin-and-tube heat exchanger surfaces. *J Therm Sci Eng Appl* 2017;9. <https://doi.org/10.1115/1.4035925>.
- [78] Armengol JM, Salinas CT, Xamán J, Ismail KAR. Modeling of frost formation over parallel cold plates considering a two-dimensional growth rate. *Int J Therm Sci* 2016;104:245–56. <https://doi.org/10.1016/J.IJTHERMALSCI.2016.01.017>.
- [79] Lee J, Kim J, Kim DR, Lee K-S. Modeling of frost layer growth considering frost porosity. *Int J Heat Mass Transf* 2018;126:980–8. <https://doi.org/10.1016/j.ijheatmasstransfer.2018.05.098>.
- [80] Kondepudi SN, O’Neal DL. Frosting performance of tube fin heat exchangers with wavy and corrugated fins. *Exp Therm Fluid Sci* 1991;4:613–8. [https://doi.org/10.1016/0894-1777\(91\)90040-X](https://doi.org/10.1016/0894-1777(91)90040-X).
- [81] Le Gall R, Grillot JM, Jallut C. Modelling of frost growth and densification. *Int J Heat Mass Transf* 1997;40:3177–87. [https://doi.org/10.1016/S0017-9310\(96\)00359-6](https://doi.org/10.1016/S0017-9310(96)00359-6).
- [82] Fukada S, Inoue K. Internal mass flux through frost. *AIChE J* 1999;45:2646–52. <https://doi.org/10.1002/aic.690451221>.

- [83] Lee YB, Ro ST. Analysis of the frost growth on a flat plate by simple models of saturation and supersaturation. *Exp Therm Fluid Sci* 2005;29:685–96.  
<https://doi.org/10.1016/j.expthermflusci.2004.11.001>.
- [84] Tahavvor AR, Yaghoubi M. Experimental and numerical study of frost formation by natural convection over a cold horizontal circular cylinder. *Int J Refrig* 2010;33:1444–58.  
<https://doi.org/10.1016/j.ijrefrig.2010.06.004>.
- [85] Kandula M. Frost growth and densification in laminar flow over flat surfaces. *Int J Heat Mass Transf* 2011;54:3719–31.
- [86] Tso CP, Cheng YC, Lai ACK. An improved model for predicting performance of finned tube heat exchanger under frosting condition, with frost thickness variation along fin. *Appl Therm Eng* 2006;26:111–20. <https://doi.org/10.1016/J.APPLTHERMALENG.2005.04.009>.
- [87] Brèque F, Nemer M. Frosting modeling on a cold flat plate: Comparison of the different assumptions and impacts on frost growth predictions. *Int J Refrig* 2016;69:340–60.  
<https://doi.org/10.1016/J.IJREFRIG.2016.06.010>.
- [88] Yao Y, Jiang Y, Deng S, Ma Z. A study on the performance of the airside heat exchanger under frosting in an air source heat pump water heater/chiller unit. *Int J Heat Mass Transf* 2004;47:3745–56. <https://doi.org/10.1016/j.ijheatmasstransfer.2004.03.013>.
- [89] Mulot V, Benkhalifa H, Pathier D, Ndoye FT, Flick D. Measurement of food dehydration during freezing in mechanical and cryogenic freezing conditions. *Int J Refrig* 2019;103:329–38. <https://doi.org/10.1016/j.ijrefrig.2019.02.032>.
- [90] Ashby B, James G, Kramer A. Effects of freezing end packagind methods on shrinkage of hams in frozen storage. *J Food Sci* 1973;38:254–7.  
<https://doi.org/10.1111/j.1365-2621.1973.tb01398.x>.
- [91] Schmidt SJ, Lee JW. How Does the Freezer Burn Our Food? *J Food Sci Educ* 2009;8:45–52.  
<https://doi.org/10.1111/j.1541-4329.2009.00072.x>.
- [92] Franks F. Freeze-drying of bioproducts: putting principles into practice. *Eur J Pharm Biopharm*; 1998;45:221-229. [https://doi.org/10.1016/S0939-6411\(98\)00004-6](https://doi.org/10.1016/S0939-6411(98)00004-6).
- [93] Phimolsiripol Y, Love R., Cleland D. Verification of a simple product weight loss model for refrigerated storage of foods. *Proc. Third IIR Int. Conf. Sustain. Cold Chain*. London, 2014.
- [94] Landerslev MG, Araya-Morice A, Pomponio L, Ruiz-Carrascal J. Weight loss in superchilled pork as affected by cooling rate. *J Food Eng* 2018;219:25–8.  
<https://doi.org/10.1016/J.JFOODENG.2017.09.012>.

- [95] Campañone LA, Salvadori VO, Mascheroni RH. Weight loss during freezing and storage of unpackaged foods. *J Food Eng* 2001;47:69–79. [https://doi.org/10.1016/S0260-8774\(00\)00101-1](https://doi.org/10.1016/S0260-8774(00)00101-1).
- [96] Powell RW. Further experiments on the evaporation of water from saturated surfaces. *Engineering J* 1940;150:238-280..
- [97] Laguerre O, Flick D. Frost formation on frozen products preserved in domestic freezers. *J Food Eng* 2007;79:124–36. <https://doi.org/10.1016/J.JFOODENG.2006.01.036>.
- [98] Bustabad OM. Weight loss during freezing and the storage of frozen meat. *J Food Eng* 1999;41:1–11. [https://doi.org/10.1016/S0260-8774\(99\)00065-5](https://doi.org/10.1016/S0260-8774(99)00065-5).
- [99] Martins RC, Almeida MG, Silva CLM. The effect of home storage conditions and packaging materials on the quality of frozen green beans. *Int J Refrig* 2004;27:850–61. <https://doi.org/10.1016/J.IJREFRIG.2004.04.008>.
- [100] Doytcheva B, Nikolova A, Peev G, Todorova D. Mass transfer from a single grain to a fluid in an inert fixed bed. *Int Commun Heat Mass Transf* 1998;25:399–405. [https://doi.org/10.1016/S0735-1933\(98\)00027-X](https://doi.org/10.1016/S0735-1933(98)00027-X).
- [101] Tocci AM, Mascheroni RH. Heat and mass transfer coefficients during the refrigeration, freezing and storage of meats, meat products and analogues. *J Food Eng* 1995;26:147–60. [https://doi.org/10.1016/0260-8774\(94\)00046-C](https://doi.org/10.1016/0260-8774(94)00046-C).
- [102] Widell KN. Energy efficiency of freezing tunnels. Norwegian University of Science and Technology. Department of Energy and process Engineering. Trondheim; 2012 (Thesis).
- [103] Buisard G. Le traitement des surgelateurs et congelateurs en industries agro alimentaires 2011:25–7. Available from <http://gbuisard.chez.com/main7.html>; 2011 [accessed 11 jbruary 2021]
- [104] Lang GD, Gasteyer TH, Ho, YCS. Impingement cooler. Eur Patent Office; 1999. <https://data.epo.org/gpi/EP0986966A2>
- [105] Smith G. Theoretical cooling coil calculations at freezer temperatures to avoid unfavourable coil frost. *ASHRAE Trans* 1989;95:1138–48.
- [106] Smith G. Latent heat, equipment-related load, and applied psychrometrics at freezer temperatures. *ASHRAE Trans* 1998;98:649–57.
- [107] Reindl DT. Defrosting industrial refrigeration evaporators. *ASHRAE J* 2009;51.

- [108] Deng DQ, Xu L, Xu SQ. Experimental investigation on the performance of air cooler under frosting conditions. *Appl Therm Eng* 2003;23:905–12. [https://doi.org/10.1016/S1359-4311\(03\)00022-X](https://doi.org/10.1016/S1359-4311(03)00022-X).
- [109] Aljuwayhel NF, Reindl DT, Klein SA, Nellis GF. Experimental investigation of the performance of industrial evaporator coils operating under frosting conditions. *Int J Refrig* 2008;31:98–106. <https://doi.org/10.1016/j.ijrefrig.2007.05.010>.
- [110] Xia Y, Zhong Y, Hrnjak PS, Jacobi AM. Frost, defrost, and refrost and its impact on the air-side thermal-hydraulic performance of louvered-fin, flat-tube heat exchangers. *Int J Refrig* 2006;29:1066–79. <https://doi.org/10.1016/j.ijrefrig.2006.03.005>.
- [111] Chen H, Thomas L, Besant RW. Modeling frost characteristics on heat exchanger fins: Part I. Numerical model. *ASHRAE Trans* 2000;106:368–76.
- [112] Wagner WB. Frost formation on a Extended Surface Heat Exchanger in Crossflow of Humid Air. Ohio State University, 1963 (Thesis).
- [113] Rite RW, Crawford RR. The Effect of Frosting on the Performance of Domestic Refrigerator-Freezer Finned Tube Evaporator Coils. Illinois University, 1990 (Thesis).
- [114] O'Hagan AN. The Effect of Favourable and Unfavourable Frost on Air Cooling coil performance. Massey University; 1994 (Thesis).
- [115] Gatchilov T, Ivanova V. Characteristics of the frost formed on the surface of the finned air coolers. XV Int. Congr. Refrig. Venice, 1979.
- [116] Gin B, Farid MM, Bansal PK. Effect of door opening and defrost cycle on a freezer with phase change panels. *Energy Convers Manag* 2010;51:2698–706. <https://doi.org/10.1016/J.ENCONMAN.2010.06.005>.
- [117] Zhao R, Huang D, Zhang Z, Leng Y. Effect of defrost heat leakage on freezer temperature rise during periodical defrost cycles in a frost-free refrigerator–freezer with an electric defrost heater. *Sci Technol Built Environ* 2017;23:211–7. <https://doi.org/10.1080/23744731.2016.1210972>.
- [118] Gaspar P, Silva PD. Handbook of research on advances and applications in refrigeration systems and technologies.2015. DOI: 10.4018/978-1-4666-8398-3
- [119] Amer M, Wang C, Amer M, Wang C. Review of defrosting methods. *Renew Sustain Energy Rev* 2017;73:53–74. <https://doi.org/10.1016/j.rser.2017.01.120>.
- [120] Hoffenbecker N, Klein SA, Reindl DT. Hot gas defrost model development and validation. *Int J Refrig* 2005;28:605–15. <https://doi.org/10.1016/J.IJREFRIG.2004.08.016>.

- [121] Dopazo JA, Fernandez J, Uhia FJ, Diz R. Modelling and experimental validation of the hot-gas defrost process of an air-cooled evaporator. *Int J Refrig* 2010;33:829–39.  
<https://doi.org/10.1016/j.ijrefrig.2009.12.027>.
- [122] Niederer DH. Frosting and Defrosting Effects on Coil Heat Transfer. *ASHRAE Trans* 1976;82:467–73.
- [123] Cole RA. Refrigeration loads in a freezer due to hot gas defrost and their associated costs, *ASHRAE Transactions* 95(2); 1989, p. 1149–1154.
- [124] Pu L, Liu R, Huang H, Zhang S, Qi Z, Xu W, et al. Experimental study of cyclic frosting and defrosting on microchannel heat exchangers with different coatings. *Energy Build* 2020;226:110382.  
<https://doi.org/10.1016/j.enbuild.2020.110382>.
- [125] Wang F, Liang C, Yang M, Fan C, Zhang X. Effects of surface characteristic on frosting and defrosting behaviors of fin-tube heat exchangers. *Appl Therm Eng* 2015;75:1126–32.  
<https://doi.org/10.1016/j.applthermaleng.2014.10.090>.
- [126] Heu CS, Kim SW, Kim J, Lee S, Kim JM, Lee K-S, et al. Frosting and defrosting behavior of slippery surfaces and utilization of mechanical vibration to enhance defrosting performance. *Int J Heat Mass Transf* 2018;125:858–65.  
<https://doi.org/10.1016/J.IJHEATMASSTRANSFER.2018.04.146>.
- [127] Cai L, Wang R, Hou P, Zhang X. Study on restraining frost growth at initial stage by hydrophobic coating and hygroscopic coating. *Energy Build* 2011;43:1159–63.  
<https://doi.org/10.1016/j.enbuild.2010.09.012>.
- [128] Liu Z, Wang H, Zhang X, Meng S, Ma C. An experimental study on minimizing frost deposition on a cold surface under natural convection conditions by use of a novel anti-frosting paint. Part II. Long-term performance, frost layer observation and mechanism analysis. *Int J Refrig* 2006;29:237–42. <https://doi.org/10.1016/J.IJREFRIG.2005.05.017>.
- [129] Joppolo CM, Molinaroli L, De Antonellis S, Merlo U. Experimental analysis of frost formation with the presence of an electric field on fin and tube evaporator. *Int J Refrig* 2012;35:468–74.  
<https://doi.org/10.1016/j.ijrefrig.2011.10.017>.
- [130] Wang D, Tao T, Xu G, Luo A, Kang S. Experimental study on frosting suppression for a finned-tube evaporator using ultrasonic vibration. *Exp Therm Fluid Sci* 2012;36:1–11.  
<https://doi.org/10.1016/j.expthermflusci.2011.03.002>.
- [131] Lee K-S, Kim W-S. The effects of design and operating factors on the frost growth and thermal

- performance of a flat plate fin-tube heat exchanger under the frosting condition. *KSME Int J* 1999;13:973–81. <https://doi.org/10.1007/BF03184764>.
- [132] Silva DL, Hermes CJL. Optimal defrost cycle for air coolers revisited: A study of fan-supplied tube-fin evaporators. *Int J Refrig* 2018. <https://doi.org/10.1016/j.ijrefrig.2018.02.009>.
- [133] Shao L-L, Yang L, Zhang C-L. Comparison of heat pump performance using fin-and-tube and microchannel heat exchangers under frost conditions. *Appl Energy* 2010;87:1187–97.
- [134] Kim K, Lee KS. Frosting and defrosting characteristics of surface-treated louvered-fin heat exchangers: Effects of fin pitch and experimental conditions. *Int J Heat Mass Transf* 2013;60:505–11. <https://doi.org/10.1016/j.ijheatmasstransfer.2013.01.036>.
- [135] Jiang Y, Dong J, Qu M, Deng S, Yao Y. A novel defrosting control method based on the degree of refrigerant superheat for air source heat pumps. *Int J Refrig* 2013;36:2278–88. <https://doi.org/10.1016/j.ijrefrig.2013.05.016>.
- [136] Buick TR, McMullan JT, Morgan R, Murray RB. Ice detection in heat pumps and coolers. *Int J Energy Res* 1978;2:85–98. <https://doi.org/10.1002/er.4440020109>.
- [137] Li X, Li Y, Seem JE. International Refrigeration and Air Conditioning Conference. Paper 1094. International Refrigeration and Air Conditioning Conference at Purdue. 2010.
- [138] Maldonado JM, de Gracia A, Zsembinszki G, Moreno P, Albets X, González MÁ, et al. Frost detection method on evaporator in vapour compression systems. *Int J Refrig* 2020;110:75–82. <https://doi.org/10.1016/j.ijrefrig.2019.10.023>.
- [139] Cleland DJ. Unfavorable frost - What is it, when does it occur and how can it be avoided, *Australien Insit Refrig. Ecolibrium*, 2004;2:16–20.
- [140] Chen H. Modeling and Measurement of Frost Characteristics on Heat Exchanger Surfaces. University of Saskatchewan; 2000 (Thesis). <https://doi.org/10.1016/b978-012397720-5.50034-7>.
- [141] Wang SW, Liu ZY. A new method for preventing HP from frosting. *Renew Energy* 2005;30:753–61. <https://doi.org/10.1016/J.RENENE.2003.07.001>.
- [142] Zhang L, Fujinawa T, Saikawa M. Theoretical study on a frost-free household refrigerator-freezer. *Int J Refrig* 2016;62:60–71. <https://doi.org/10.1016/J.IJREFRIG.2015.10.008>.
- [143] Wang Z, Zheng Y, Wang F, Wang X, Lin Z, Li J, et al. Experimental analysis on a novel frost-free air-source heat pump water heater system. *Appl Therm Eng* 2014;70:808–16. <https://doi.org/10.1016/J.APPLTHERMALENG.2014.05.038>.

- [144] Vivekh P, Kumja M, Bui DT, Chua KJ. Recent developments in solid desiccant coated heat exchangers – A review. *Appl Energy* 2018;229:778–803.  
<https://doi.org/10.1016/J.APENERGY.2018.08.041>.
- [145] Thierry DB, Didier P. Systeme ameliorant les problemes de givrage dans les tunnels de surgelation par impaction. Patent WO/2013/050680;2012.  
<https://patentscope.wipo.int/search/fr/detail.jsf?docId=WO2013050680>